

# Debris Avoidance in Low Earth Orbit

Jyoshika Barathimogan, Leow Eason, Helen Chen

**Abstract** - The exponential growth of Low Earth Orbit (LEO) satellites has increased the risk of collisions and the creation of long-lived debris. Today, conjunction assessments and collision avoidance manoeuvres (CAMs) are ground-controlled, causing delays, fuel inefficiencies, and mission disruptions. The Copernicus Sentinel-1A satellite, launched in 2014, has already experienced debris impacts and multiple CAMs, leading to data losses and reduced efficiency.

This proposal introduces DAWN (Debris-Aware Autonomy Node), a retrofittable on-board AI system to enhance operational resilience. DAWN integrates Graph Neural Networks for debris trajectory prediction, Reinforcement Learning with Chance-Constrained Model Predictive Control for manoeuvre planning, and lightweight computer vision for object classification. An end-of-life deorbit scheduler ensures safe orbital exit.

By retrofitting Sentinel-1A, DAWN demonstrates how AI-driven autonomy can reduce operator workload, minimise downtime, and establish a template for future autonomous Earth-observation satellites in crowded orbital environments.

## I. INTRODUCTION

### Literature Review

Low Earth Orbit (LEO) is becoming more crowded with satellites, and this congestion has increased the risk of conjunctions and collisions with space debris. This growing problem threatens space-based infrastructure, with the potential to create a chain reaction of further collisions, a Kessler effect. Previous incidents, such as the 2009 Iridium–Cosmos collision [1] and China's 2007 anti-satellite test [2], produced thousands of fragments that remain in orbit,

demonstrating how debris can persist for decades and continue to pose risks.

The Copernicus Sentinel-1A satellite, launched in 2014, provides Synthetic Aperture Radar (SAR) data for environmental monitoring, maritime surveillance, and disaster response. Sentinel-1A has experienced several debris-related events. In August 2016, it was struck by a small debris particle, which damaged its solar panel wing and caused a small power reduction and minor attitude disturbances [3]. More recently, in August 2025, Sentinel-1A suffered a technical anomaly that led to the permanent loss of part of its data service, highlighting its vulnerability to disruptions [4]. In addition to direct impacts, Sentinel-1A has performed multiple CAMs that interrupted SAR imaging and created temporary data gaps [5][6].

Currently, collision risk is managed by using ground-based orbital catalogues, such as Two-Line Elements (TLEs) provided by the U.S. Space Command. These data are useful but uncertain when it comes to small debris fragments that cannot be tracked consistently. CAM decisions are planned and executed on Earth, then uplinked to the satellite. This approach is heavily reliant on human intervention, consumes time and remains vulnerable to mission disruption.

### State of the Art of DAWN

Recent research has explored artificial intelligence to improve different aspects of space situational awareness, but applications remain in development. Machine learning models have been tested for classifying conjunction alerts and filtering false positives [7], while reinforcement learning

# Debris Avoidance in Low Earth Orbit

Jyoshika Barathimogan, Leow Eason, Helen Chen

approaches have been simulated for manoeuvre planning [8]. Advances in computer vision, such as event-based imaging, show potential for classifying nearby space objects when detected in orbit.

However, no operational satellite like Sentinel-1A hosts an on-board edge AI system capable of autonomously predicting debris trajectories, planning CAMs, and selecting safe deorbit windows. Still, ground-based solutions dominate current practice, leaving a gap in autonomy that could be filled by AI-enabled systems.

## Proposed Solution

This project introduces DAWN (Debris-Aware Autonomy Node) as a retrofittable AI-enabled module for Sentinel-1A.

The objectives are:

Autonomous debris trajectory prediction that uses orbital mechanics with Graph Neural Networks (GNNs) to predict debris paths under uncertainty.

Fuel-optimal manoeuvre planning that leverages Reinforcement Learning (RL) together with Chance-Constrained Model Predictive Control (CC-MPC) to compute safe CAMs while minimising fuel use.

On-board object classification that will integrate a lightweight computer vision model to identify nearby debris objects, supporting situational awareness while gathering data for manoeuvre and prediction.

End-of-life sustainability that schedules safe deorbit windows to avoid congested orbital shells to reduce long-term debris risk.

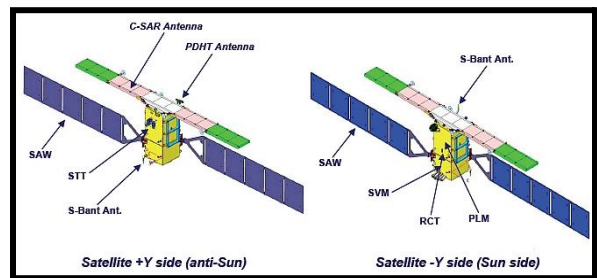
Through these objectives, DAWN aims to show how Sentinel-1A can be fitted with autonomy that reduces operator workload, minimises downtime, and sets a foundation for next-generation Earth-observation missions or the next Sentinel.

## II. MISSION SPECIFICATION

### Mission objective

We plan to enhance Copernicus Sentinel-1A with a retrofit AI module (DAWN) for real time autonomy collision avoidance.

Copernicus Sentinel-1A



(Copernicus Sentinel-1A Credits: TAS-I)

### Sentinel-1A description

Sentinel-1A was launched on 3 April 2014 as part of the Copernicus program managed by the European Space Agency (ESA). Its main missions consist of environment monitoring such as land, marine, iceberg monitoring and emergency mapping support during natural disasters. Its planned service duration is 7 years with consumables for 12 years, now it's still in service.

Sentinel-1A is three axis stabilized (yaw/pitch/roll steering) with  $0.01^\circ$  altitude accuracies on each axis. It was also equipped with two 8-channel GPS to determine its real time orbit. The two 8-channel GPS use dual-frequency GPS measurements to collect orbit data. The data

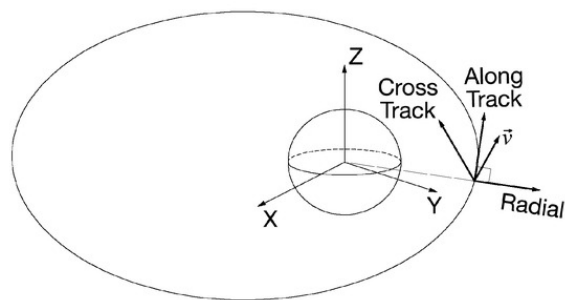
# Debris Avoidance in Low Earth Orbit

Jyoshika Barathimogan, Leow Eason, Helen Chen

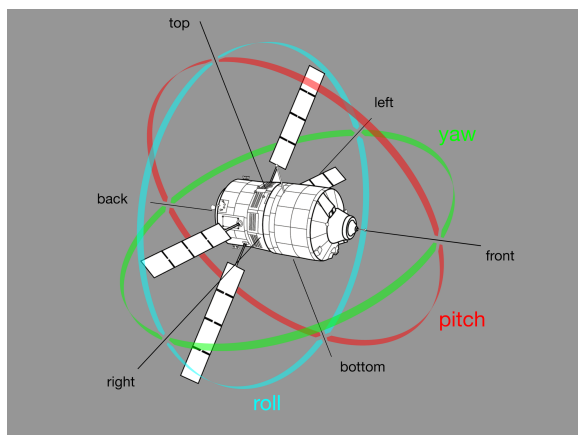
was then handled by the Copernicus Precise Orbit Determination (CPOD) service to refine the satellite's trajectory, fulfilling the 5 cm 3D orbit accuracy (satellite's position in space in all three directions: radial, along-track, and cross-track) required for its radar mission. [9]

## Roll, pitch, yaw (orientation) vs radial, along-track, cross-track (translation)

Roll, pitch, and yaw refer to the control of which way it points in space; radial, along-track, cross-track refer to the position of satellites in the orbits.



(Credits: [Conceptual diagram to show the definition of the radial, in-track,...](#) | [Download Scientific Diagram](#))



(Credits: [Shining light on ATV – Orion blog](#) )

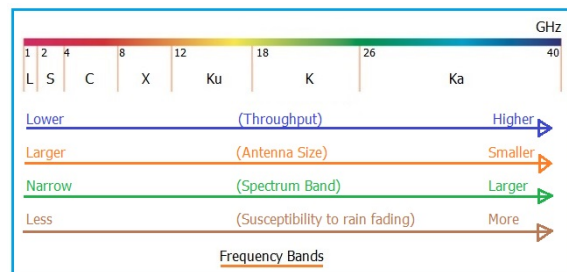
## Orbit

Sentinel-1A is in a sun-synchronous, near polar and circular orbit with 693km altitude. The period of its orbit is 98.6 minutes, it's also a 12-day repeat cycle at Equator (meaning it revisits the same location on the Equator every 12 days). [10]

## Infrastructure of Sentinel-1A

The total mass of Sentinel-1A is 2300kg, with 130kg as fuel. It communicate with ground via X-band data downlink, Optical data link through European Data Relay Satellite System (EDRS), S-band 64 kbps uplink and 128 kbps / 2 Mbps downlink for TM/TC. [11]

X-band data downlink & S-band uplink and downlink: It refers to the transmission of data from satellite to ground station, using radio waves in the X-band frequency (downlink). Transmission of data from ground station to satellite using S-band frequency (uplink), transmission of data from satellite to ground using S-band frequency (downlink) for telemetry and telecommand (TM/TC).



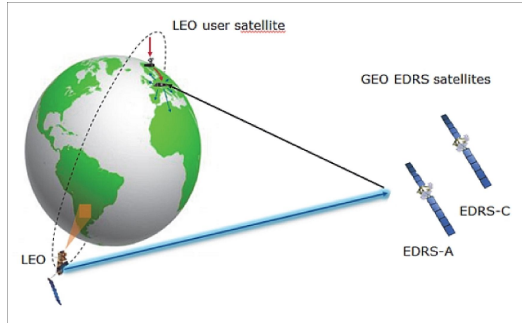
(X-band and S-band frequency credits: [X Band Frequency: Values, Advantages, and Applications | RF Wireless World](#) )

Optical data link through EDRS: optical data link uses laser instead of radio waves (like X-band or S-band) to transmit data,

# Debris Avoidance in Low Earth Orbit

Jyoshika Barathimogan, Leow Eason, Helen Chen

Sentinel-1A will use laser to transmit data to EDRS satellites in GEO, EDRS satellite then forwards the data to a ground station



(EDRS credits: [EDRS - eoPortal](#))

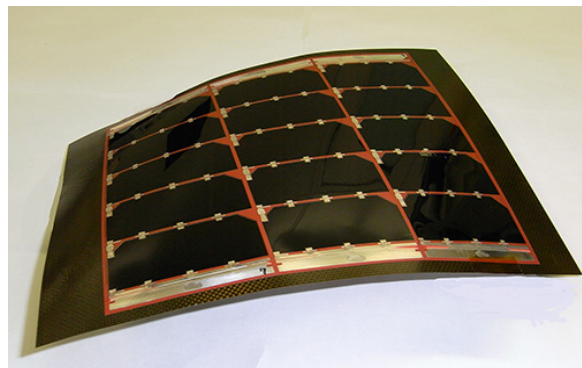
The satellite platform (also called spacecraft bus, is the infrastructure of the satellite) used for Sentinel-1A is called PRIMA bus (Piattaforma Italiana Multi Applicativa). It consists of three modules:

- (1) service module (SVM)
  - (2) propulsion module (PPM)
  - (3) payload module (PLM).
- (1) service module (SVM) consists of various subsystems.

Thermal Control Subsystem (TCS) controls the satellite's temperature. It is mainly passive thermal control using multi-layer insulation, heat pipes, radiator and survival heater [12]

Electric Power Subsystem (EPS) manages solar arrays, batteries, and power distribution. EPS consisted of two deployable solar arrays (providing about 5900 W at end of life), each with 5 sandwich panels using GaAs triple-junction solar cells, and a modular battery with Li-ion technology (capacity of 324 Ah for energy storage, max discharge power  $\geq 1950$  W).

Average onboard power consumption is 4800 W at end of life. [13]



(GaAs triple-junction solar cells Credits: [Triple-junction \(InGaP/GaAs/InGaAs\) Solar Cell Sheet \(glass type\) | satsearch](#) )

Avionics Subsystem (AVS) handles data management and attitude/orbit control.

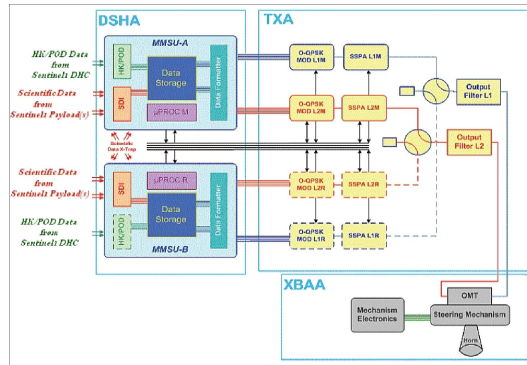
Avionics Subsystem (AVS) on Sentinel-1A integrates both data handling and attitude/orbit control functions, managing telemetry/telecommands (TM/TC), monitoring subsystem, data storage, and autonomous switching, while working with Attitude and Orbit Control Subsystem (AOCS) sensors such as star trackers, gyroscopes, sun sensor, magnetometers, GPS and actuators (device that adjust orientation or position) such as 4 reaction wheels, 3 torque rods, 14 thrusters (using hydrazine), and 2 solar array drives. AOCS provides orientation and orbit manoeuvring throughout the mission. [14]

Payload Data Handling and Transmission Subsystem (PDHT) stores and transmits payload data. It includes three main assemblies: Telemetry X-band Transmission Assembly (TXA), X-Band Antenna Assembly (XBAA), Data Storage & Handling Assembly (DSHA).

# Debris Avoidance in Low Earth Orbit

Jyoshika Barathimogan, Leow Eason, Helen Chen

DSHA (with data storage capacity of 1410 Gbit at end of life) temporarily stores data from the C-SAR, organizes it, and sends it to the TXA. TXA then prepares payload data for X-band transmission to the ground. Upon receiving the observation data from the DSHA, TXA modified it and sent it to XBAA. TXA has two X-band channels , each with 16 dBW output power and up to 260 Mbit/s useful data rate. The main components of TXA are X-band modulators which generate the modulated data signal , Traveling Wave Tube Amplifiers (TWTA) which amplify the signal up to 60 W radio frequency power and Optical Multiplexer (OMUX) which ensuring clean signals and rejecting unwanted frequencies. Upon receiving the X-band signal from the TXA, XBAA radiates it through a wide-coverage isoflux antenna to ground. [15]



(PDHT Subsystem Credits: TAS-I  
[Copernicus: Sentinel-1 - eoPortal](#))

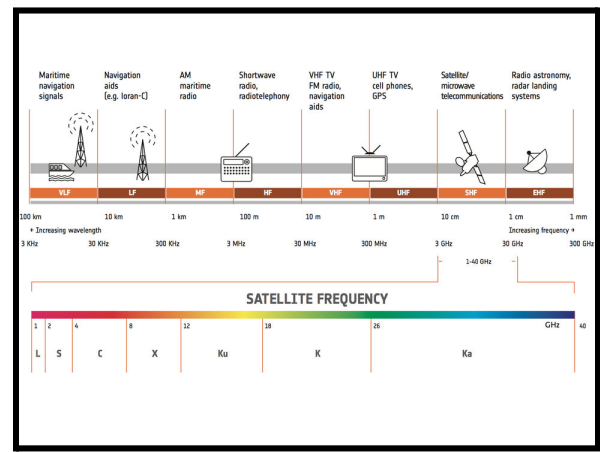
**Propulsion Subsystem (PRP):** controls satellite's orbit and attitude using thrusters and propellant. Consists of 14 Reaction Control Thrusters (RCT)

(2) propulsion module (PPM) carrying all the propulsion items: including propellant tanks, pipes and tubings, and 14 thrusters.

(3) payload module (PLM) carrying C-band Synthetic Aperture Radar (C-SAR), which is the primary sensor used for earth observation, and some supporting electronics.

## Sentinel-1A Payload

Sentinel-1A carries a C-band Synthetic Aperture Radar (C-SAR). It allows all weather, all day and night imagery. It's because SAR can transmit its own microwave signal towards the earth, receiving part of the reflected signal to be used for image construction. C-band SAR operate in frequency around 4-8GHz, wavelength around 5.6cm. It offers good image resolution while maintaining the penetration capabilities.



(Satellite frequency chart Credits: ESA Satellite frequency band)

Sentinel-1A C-SAR can transmit and receive signals in horizontal (H) or vertical polarization (V). polarization of electromagnetic waves is defined by the direction its electric field oscillates, either horizontal or vertical. There is commonly four types of polarization used: Horizontal transmit Horizontal receive (HH), Vertical

# Debris Avoidance in Low Earth Orbit

Jyoshika Barathimogan, Leow Eason, Helen Chen

transmit Vertical receive (VV), Vertical transmit Horizontal receive (VH), Horizontal receive Vertical transmit (HV) [16]

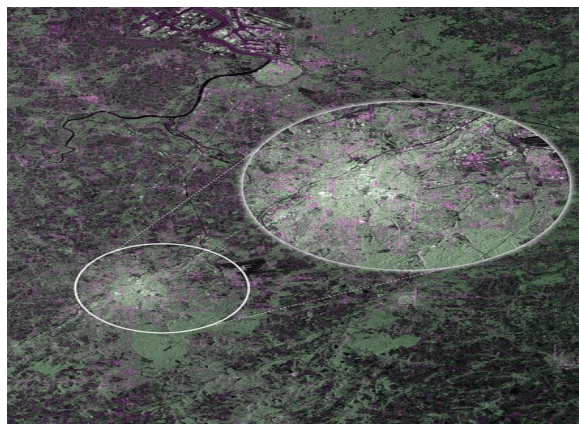
Sentinel-1A C-SAR support two types of polarization mode :

- I. Single polarization: HH or VV
- II. Dual polarization: HH+HV or VV+VH

Sentinel-1A C-SAR is designed to be able to run in four modes:

- 1) Stripmap mode (SM): single or dual polarization
- 2) Interferometric Wide Swath mode (IWS): single or dual polarization
- 3) Extra Wide Swath mode (EWS): single or dual polarization
- 4) Wave mode (WM): single polarization

[17]

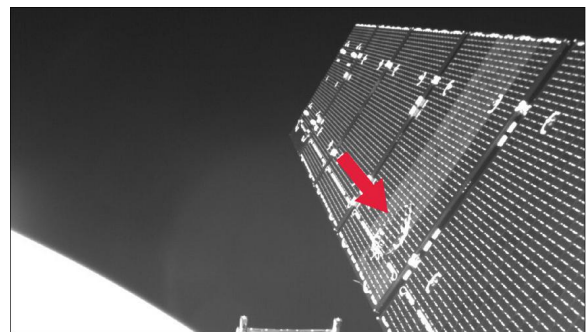


(First image by Sentinel-1A C-SAR in SM dual polarization mode Credits: ESA)

Sentinel-1A collision with space debris

On 23 August 2016, Sentinel-1A suffered a collision with space debris on one of its solar arrays, causing a small power reduction and slight change in orientation and orbit of sentinel-1A. ESA's teams are

able to detect the impact area using onboard cameras, luckily the power reduction is small and Sentinel-1A able to remain in operation [18]. In August 2025 recently, Sentinel-1A suffered permanent data loss of the data recorded on August 10 due to system anomaly.



(Sentinel-1A collide with space debris  
Credits : [Copernicus: Sentinel-1 - eoPortal](#))

## Dawn system function

DAWN will process the space debris data input with Graph Neural Networks (GNNs), make decisions with Reinforcement Learning (RL) and Chance-Constrained Model Predictive Control (CC-MPC) for collision avoidance.

## Data input

The source of space debris data can be classified into two types: 1) data from ground: TLEs, radar, optical observations 2) data from onboard: lightweight computer vision models. TLEs stands for two-line element set. It is a data format that describes the orbital elements of an earth orbiting object [19], which can be used to describe the position and trajectories of earth orbiting objects such as satellites and space debris. However, TLEs are inaccurate for collision avoidance maneuver [20].

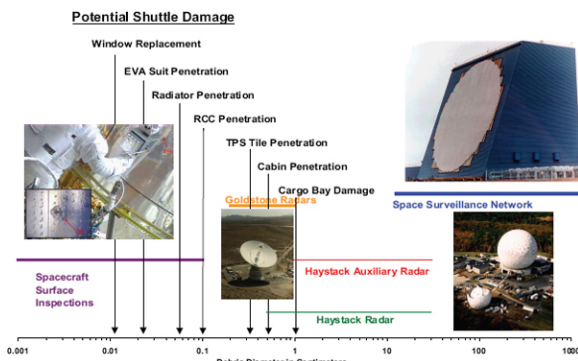
# Debris Avoidance in Low Earth Orbit

Jyoshika Barathimogan, Leow Eason, Helen Chen

COSMOS 2251	1 22675U 93036A	25271.98651171	.00000242	00000+0	97255-4 0	9997
2	22675	74.0375	92.4641	0025121	197.7087	162.3191 14.33170402687027

(TLEs data of one of the cosmos 2251 satellite debris  
credit: Celestrak: COSMOS 2251 Debris)

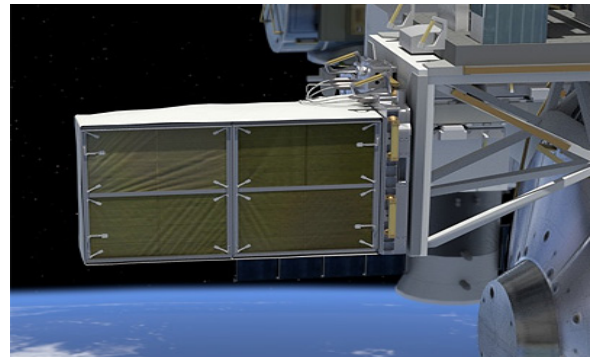
For radar and optical observations, Radar such as Weibel's long-range tracking radar systems, space surveillance radar GESTRA and LeoLabs PAFR radars are used for tracking space objects such as space debris. [21] Radars like LeoLabs PAFR and Weibel's long-range tracking radar systems can track space debris with a diameter  $>10$  cm in Low Earth Orbit (LEO). However, radar systems only catalog the amount of space debris, not tracking them. They also have limitations such as position limitation and not being able to track space debris that are in Molniya-type orbit. [22]



(LEO space debris measurement capability credit: [2 Orbital Debris Environment: Detection and Monitoring | Limiting Future Collision Risk to Spacecraft: An Assessment of NASA's Meteoroid and Orbital Debris Programs | The National Academies Press](#))

For onboard space debris monitoring, NASA developed a space debris sensor called NASA's Space Debris Sensor (SDS) that can be installed outside of ISS station to monitor space debris of size between 5 mm to 0.5

mm in diameter, which can't be tracked by ground radar and telescope. [23] It consists of three layers, the first and second layers measure debris size, impact location and time, the last layer measures the impact energy. [24]



(Picture of SDS mounted outside of ISS  
Credits: [SDS - Gunter's Space Page](#))

## AI models

GNNs is a type of neural network that works with graph-structured data. It's suitable for predicting debris trajectories because space debris interactions are graph-like problems. It's done by "representing each object as a node in the graph and defining the edges based on the objects' spatial proximity, quantified by the orbit altitude differences".[25] RL is a type of machine learning that lets machines interact with the environment, receive feedback to improve their decision making in the future. It's suitable for satellites because the satellite must make decisions in dynamic and uncertain environments (space), it allows the satellite to learn from experience, optimising safety and fuel efficiency manoeuvres while avoiding collisions. CC-MPC is a control strategy that combines predictive planning with probabilistic safety constraints. It's because there are always uncertainties in

# Debris Avoidance in Low Earth Orbit

Jyoshika Barathimogan, Leow Eason, Helen Chen

space debris trajectory; therefore, CC-MPC sets an “upper bound” for the collision probability, ensuring the collision avoidance maneuver below a fixed limit of collision probability [26].

RL proposes manoeuvres based on learned strategies for efficiency and safety. CC-MPC acts as a safety filter, rejecting manoeuvres that exceed the allowed collision probability. Together, this ensures that autonomous manoeuvres are both fuel-efficient and safe.

### III. SOLUTION Analysis

The proposed DAWN solution is designed as a retrofittable on-board module that addresses the current shortcomings of ground-controlled collision avoidance practices. While traditional systems depend on delayed ground commands, DAWN shifts its decision-making onto the spacecraft itself, combining physics-based orbital mechanics with advanced AI methods and techniques.

#### *Autonomous debris trajectory prediction*

Conventional models such as SGP4 often accumulate uncertainty when forecasting conjunctions, specifically when debris lacks precise tracking data. While SGP4 is fast, its precision degrades due to numerical propagators over a longer prediction interval [27]

DAWN integrates *Graph Neural Networks (GNNs)* with orbital mechanics to capture the relational dynamics of debris objects within the congested orbital shells. This hybrid method is inspired by the framework used in “From Space Weather to Orbits: An Uncertainty-Aware Framework for

Predicting Satellite Trajectories” [28], which allows the satellite to adapt predictions in real time, reducing false alarms and enhancing local situational awareness.

#### *Fuel Optimal Manoeuvre Planning*

CAMs are generally conservative, prioritising safety margins, but this leads to excessive fuel usage and mission downtime. Studies show that robust optimisation, such as Linear Programming (LP) and deterministic CAM strategies, while reliable, can waste valuable propellant over long operational lifetimes [29].

DAWN addresses this inefficiency by combining RL for adaptive manoeuvre generation with CC-MPC to validate trajectories under probabilistic safety guarantees. Recent work shows that RL approaches to train agents do effectively optimize CAM strategies for fuel efficiency while maintaining a safety threshold [30], and CC-MPC frameworks have also been applied successfully in uncertain environments to ensure collision probabilities remain below acceptable limits.

By deploying lightweight, pre-trained RL policies on board and refining them through CC-MPC, DAWN uses real-time CAM planning that balances responsiveness with computational feasibility.

#### *On Board Object Classification*

Not every orbital debris has the same threat profile. Some small paint flakes may burn up harmlessly, while larger inactive satellites or fragments pose severe collision risks.

DAWN addresses this by deploying a lightweight computer vision (CV) model

# Debris Avoidance in Low Earth Orbit

Jyoshika Barathimogan, Leow Eason, Helen Chen

that classifies nearby debris captured through on-board imaging.

This also extends into situational awareness beyond catalogued objects, enabling satellites to build local datasets and improve trajectory predictions with empirical evidence. NASA’s Space Debris Sensor (SDS) has already tested the feasibility of in-orbit debris detection and classification [31], while CubeSat missions have also successfully tested vision-based navigation frameworks that inform object tracking and hazard avoidance

Despite these advantages, the approach faces challenges: small satellite processors limit the complexity of models that can be deployed, and classification errors could result in false alarms or missed threats. DAWN mitigates these risks through model compression, redundancy in sensing, and confidence-based thresholds to minimise misclassification impacts.

## Model Architecture

### *Autonomous debris trajectory prediction*

Precise debris trajectory prediction is important to help safeguard operational assets. However, current methods rely heavily on deterministic orbit propagators and ground-controlled updates. These models, like the popular SGP4 or semi-analytic propagators, can perform well under nominal conditions, but degrade significantly during geomagnetic storms and when atmospheric drag surges unpredictably.

The traditional physics-based models cannot fully account for uncertainty in space, particularly under stormy conditions where

there is drag, solar flux, and geomagnetic indices that fluctuate rapidly. At the same time, purely data-driven black-box approaches risk losing interpretability, scalability, and robustness across diverse orbital regimes. Hence, this motivates a hybrid, uncertainty-aware framework that leverages physics, while augmenting predictions with learned corrections from graph-based deep learning.

Here, we introduce an Autonomous Debris Trajectory Prediction framework that integrates with Orbital Mechanics Priors, which are baseline propagation from SGP4 and semi-analytic methods that ensure adherence to first-principles dynamics.

It integrates with Bayesian Multi-Relational Graph Convolutional Networks (MR-GCNs). As debris and satellites are modelled as nodes in a dynamic relational graph, capturing multi-relational interactions like proximity, orbital similarity, and surface properties. Bayesianization provides epistemic and aleatoric uncertainty estimates, which are important for collision avoidance.

Adding on, Space-Weather Integration like solar and geomagnetic indices (F10.7, Ap/Kp, Dst), along with empirical density models (NRLMSISE-00, JB2008), feed into the network to capture drag variability under both quiet and storm-time conditions.

The result is a predictive system that not only outputs a deterministic ephemeris, but a distributional trajectory forecast with calibrated uncertainty bounds. This design allows downstream decision modules, such as chance-constrained model predictive control (CC-MPC), to reason over risk

# Debris Avoidance in Low Earth Orbit

Jyoshika Barathimogan, Leow Eason, Helen Chen

rather than a single prediction, which helps in reducing false alarms and unnecessary collision avoidance manoeuvres while preserving fuel and mission uptime.

## High-level design

The proposed framework for Autonomous Debris Trajectory Prediction combines physics-based orbit propagation with a Bayesian multi-relational graph neural network (MR-GCN) and a temporal forecaster.

## Input

At each update cycle, define the model input as:

$$\mathcal{X}_t = \{\mathbf{s}_{t-W:t}, \mathbf{w}_{t-W:t}, \mathbf{d}_{t-W:t}, \mathbf{n}_{t-W:t}\}$$

Orbital state history (st-W:t) that osculating Keplerian elements, supplemented with velocity (s), area-to-mass ratio ( A/m) and attitude flags. Space weather input (Wt - W:t): solar and geomagnetic indices including F10.7, F10.7a, Ap, Kp, and Dst, as well as short-term forecasts from SWPC.

Density priors (dt-W:t): thermospheric density profiles sampled from empirical models (NRLMSISE-00, JB2008) along candidate trajectories.

Neighbourhood cues (nt-W:t): relational signals such as orbital similarity, spatial proximity, and operator class, which define edges in the multi-relational graph.

## Orbital Propagation

Baseline propagation is performed using SGP4 or semi-analytic propagators. For each object, the predicted state at horizon  $\tau$ :

$$\hat{\mathbf{x}}_{\text{phys}}(t + \tau) = f_{\text{phys}}(\mathbf{s}_t, \mathbf{w}_t, \mathbf{d}_t)$$

where  $(f_{\text{phys}})$  is the deterministic propagation function. While computationally efficient, this prior neglects storm-time drag anomalies and cross-object correlations, motivating the residual learning step.

## Bayesian Multi-Relational GCN

Construct a dynamic, multi-relational graph  $G_t = (V, E, R)$  where each debris object  $v_i \in V$  is a node, edges  $e_{ij}^r \in E$  represent relationships of type  $r \in R$ , and each relation type corresponds to Proximity, Orbital similarity, co-drag and surface class

Each node will  $v\{i\}$  will be encoded as:

$$\mathbf{h}_i^{(0)} = \phi(\mathbf{s}_i, \mathbf{w}_i, \mathbf{d}_i)$$

Multi-relational message passing updates node embeddings as:

$$\mathbf{h}_i^{(l+1)} = \sigma \left( \sum_{r \in R} \sum_{j \in \mathcal{N}_i^r} \frac{1}{c_{i,r}} W_r \mathbf{h}_j^{(l)} + W_0 \mathbf{h}_i^{(l)} \right)$$

Where  $c\{i,r\}$  normalises neighbours,  $W\{r\}$  are relation-specific weights, and  $\sigma(\cdot)$  is a nonlinearity.

The residual state correction at horizon  $\tau$  will be modelled as a predictive distribution where Bayesianization yields epistemic uncertainty

$$\Delta \hat{\mathbf{x}}_{\text{GNN}}(t + \tau) \sim q_\theta(\cdot | \mathcal{G}_t)$$

## Temporal Forecasting

The residual outputs are passed through a temporal forecaster, such as a Temporal Convolutional Network (TCN), to model

# Debris Avoidance in Low Earth Orbit

Jyoshika Barathimogan, Leow Eason, Helen Chen

dynamics across horizons. For each horizon  $\tau$ :

$$\Delta\hat{\mathbf{x}}_{\text{seq}}(t + \tau), \log \sigma_\tau^2 = f_{\text{temp}}(\{\Delta\hat{\mathbf{x}}_{\text{GNN}}(t - k)\}_{k=1}^W)$$

This head provides a heteroscedastic variance term  $\sigma\{\tau\}^2$ , capturing aleatoric uncertainty from noisy drag conditions.

## Fusion and Output

The final prediction fuses the physics prior with the learned correction:

$$\hat{\mathbf{x}}(t + \tau) = \hat{\mathbf{x}}_{\text{phys}}(t + \tau) \oplus \Delta\hat{\mathbf{x}}_{\text{seq}}(t + \tau)$$

The predictive covariance is estimated as, where K is the number of Monte Carlo samples.:

$$\hat{\Sigma}(t + \tau) = \underbrace{\text{Var}_{k=1..K}[\Delta\hat{\mathbf{x}}_{\text{seq}}^{(k)}(t + \tau)]}_{\text{epistemic}} + \underbrace{\sigma_\tau^2 I}_{\text{aleatoric}}$$

## Calibration and Quality Assurance

The Model quality will be assessed using both accuracy and calibration metrics. CRPS (Continuous Ranked Probability Score) for distributional sharpness. ACE (Average Coverage Error) and ECE (Expected Calibration Error) for interval calibration. Stress tests under storm-focused splits to evaluate robustness when density models diverge.

## Training Objective

The model is trained as a residual predictor with probabilistic calibration. The loss combines likelihood and uncertainty regularisation.

Using Negative Log Likelihood (NLL). For each horizon  $\tau$ , the residual distribution is assumed Gaussian:

$$\Delta\mathbf{x}_{\text{true}}(t + \tau) \sim \mathcal{N}(\mu_\tau, \sigma_\tau^2 I)$$

$$\mathcal{L}_{\text{NLL}} = \sum_{\tau=1}^H \left[ \frac{1}{2} \log |\sigma_\tau^2 I| + \frac{1}{2} (\Delta\mathbf{x}_{\text{true}}(t + \tau) - \mu_\tau)^\top \sigma_\tau^{-2} (\Delta\mathbf{x}_{\text{true}}(t + \tau) - \mu_\tau) \right]$$

With Bayesian Regularisation. If variational inference is used, we add a KL term:

$$\mathcal{L}_{\text{Bayes}} = \beta \text{KL}(q_\theta(w) \parallel p(w))$$

## Training Pipeline

The model is trained on a multi-source dataset that integrates both physics-based and empirical inputs. Historical orbital states are obtained from Two-Line Elements (TLEs) and corresponding truth ephemerides from missions like GPS, SWARM, and GRACE-FO. Space weather indices are ingested from the NOAA Space Weather Prediction Center (SWPC), which includes solar flux and geomagnetic activity indicators. Thermospheric density priors are sampled along predicted trajectories using empirical models such as JB2008 and NRLMSISE-00. At each epoch, a dynamic graph is constructed, where edges represent multi-relational dependencies.

To ensure scalability across thousands of tracked objects, a hierarchical batching strategy will be employed. Objects are first partitioned by altitude shell (400 to 500 km). Within each shell, relation-specific sparse adjacency matrices are constructed to encode proximity, orbital similarity, and operator-based relations. Temporal dependencies are captured using a sliding window of length W, which provides a sequential input context for forecasting.

During each training iteration, orbital states are first propagated using SGP4 to provide a

# Debris Avoidance in Low Earth Orbit

Jyoshika Barathimogan, Leow Eason, Helen Chen

baseline physics prior,  $x^{\text{phys}}$ . A Bayesian Multi-Relational Graph Convolutional Network (MR-GCN) is then applied to estimate residual corrections and associated epistemic uncertainty. The corrected residuals are passed through a temporal forecasting module (TCN) to generate predictions across the forecast horizon.

The model parameters are optimised via stochastic gradient descent using Adam or AdamW optimisers with adaptive learning-rate scheduling. Monte Carlo dropout or even variational Bayesian layers can be applied during training to capture epistemic uncertainty. The total loss is computed as the weighted sum of negative log-likelihood (NLL), Bayesian KL regularisation, and optional physics-consistency terms. This ensures the model simultaneously minimises trajectory error while producing calibrated uncertainty estimates.

## Inference Loop

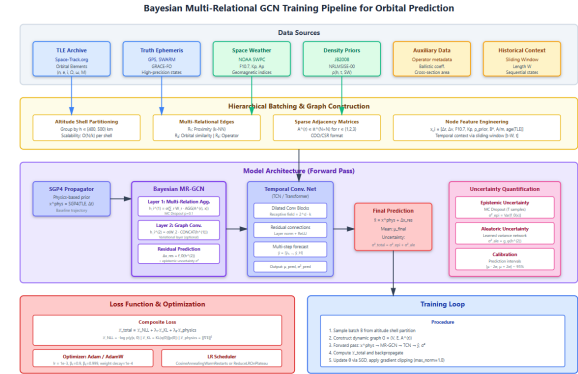
Once trained, the model operates in an autonomous inference loop to provide real-time trajectory forecasts and calibrated uncertainty estimates. The cycle is designed to run at operational cadences (every 10–30 minutes), ensuring that new space-weather updates and orbital measurements are promptly assimilated.

The cycle begins with the ingestion of new orbital measurements along with real-time space-weather indices and forecasts. These serve as the current state from which predictions will be advanced. The updated states are propagated forward using a semi-analytic propagator to provide a deterministic baseline trajectory, which acts as the physics prior for correction.

The Bayesian MR-GCN is applied to generate residual corrections, while the temporal forecaster extends these predictions across the operational horizon. During inference, multiple stochastic forward passes are performed to capture epistemic uncertainty, while the forecaster simultaneously outputs heteroscedastic variance estimates for aleatoric effects. The corrected state estimate at each horizon is obtained by fusing the deterministic prior with the residual predictions. The associated uncertainty is quantified as the combination of epistemic variance and aleatoric variance from the predictive head.

The final product is a distributional trajectory forecast, expressed as mean orbital elements and calibrated uncertainty bounds (5th–95th percentile envelopes). These outputs are packaged into a format suitable for downstream modules like chance-constrained model predictive control (CC-MPC), where decision-making relies on probability-weighted.

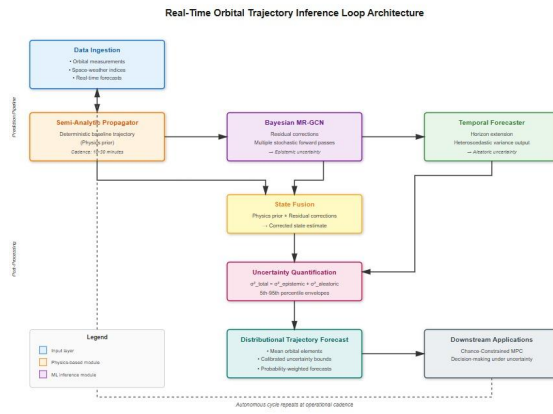
## Framework



This architecture diagram illustrates a Bayesian Multi-Relational Graph Convolutional Network (MR-GCN) training pipeline

# Debris Avoidance in Low Earth Orbit

Jyoshika Barathimogan, Leow Eason, Helen Chen



The diagram includes the autonomous feedback loop showing the operational cycle

## Evaluation Metrics

Once trained, Deterministic accuracy is measured using root mean square error (RMSE) and along-track deviation at 6, 12, and 24-hour horizons, allowing direct comparison with physics-only propagators.

Beyond point estimates, distributional quality is assessed using the Continuous Ranked Probability Score (CRPS), which balances sharpness and reliability. Calibration metrics such as Average Coverage Error (ACE) and ECE verify that predicted confidence intervals (95%) match observed frequencies.

To test robustness, evaluations are stratified by weather regime (quiet and storm periods). Finally, operational impact is measured in terms of reduced false-positive conjunction alerts and unnecessary collision avoidance manoeuvres.

## Summary

The training and inference design ensure that the system

Remains anchored in physics Also leverages relational learning across debris population.

Moreover produces distributional forecasts with calibrated uncertainty

## Fuel optimal manoeuvre planning

We formulate fuel-optimal collision-avoidance and return manoeuvres as a constrained stochastic optimal control problem over a finite horizon  $[t_0, t_f]$ .

The agent must

- keep instantaneous collision risk below a specified bound during the encounter,
- minimize propellant use ( $\Delta v$  / integrated thrust).
- restore orbital elements to nominal post-event, all under dynamics, actuator, eclipse, keep-out, and pointing constraints.

Recent work shows that uses RL is viable for low-thrust CAM return while convex and chance-constrained MPC provide strong safety with feasibility foundations hence fusing them together. RL for decision-quality and fuel efficiency, MPC for hard-safety and feasibility.

## Perception and Forecasting

The Perception and Forecasting Module provides the situational awareness that is needed for real-time decision making in low-thrust manoeuvre planning.

This integrates with navigation solutions, collision data messages (CDMs), and learned dynamical models to help construct an uncertainty-aware representation of the surrounding orbital environment. It comprises three principal components:

- Ephemerides and Covariance Estimation
- Temporal Forecasting Network
- Bayesian Multi-Relational Graph Neural Network (MR-GNN) for uncertainty propagation and risk coupling.

# Debris Avoidance in Low Earth Orbit

Jyoshika Barathimogan, Leow Eason, Helen Chen

## Ephemerides and Covariance Estimation

The onboard navigation system and periodically updated CDMs obtain the spacecraft's absolute and relative states.

Let  $x_s \in \mathbb{R}^6$  denote the satellite's position and velocity vector in the Earth-Centered Inertial (ECI) frame, and  $P_s \in \mathbb{R}^{6 \times 6}$  represent its corresponding state covariance. Similarly, for each nearby object  $i$ , the CDM provides an ephemeris  $x_i$  and covariance  $P_i$

$$\mathcal{S}_0 = \{(x_s, P_s)\} \cup \{(x_i, P_i)\}_{i=1}^N$$

where  $N$  is the number of tracked debris or resident space objects within the operational conjunction radius.

## Temporal Forecasting Network

A Temporal Convolutional Network (TCN) is trained to predict the short-term evolution of relative states and uncertainty growth.

Rather than relying only on inputting analytical propagation such as SGP4. The TCN learns residual corrections  $\hat{\Delta x}(t)$  and  $\hat{\Delta x}(P)$  over the deterministic physics model, which will improve prediction accuracy during high-drag or during perturbation-sensitive periods.

The TCN outputs the predicted relative trajectory and covariance evolution over the forecasting horizon  $[t_0, t_f]$ :

$$\{\hat{x}_{rel}(t_k), \hat{P}_{rel}(t_k)\}_{k=1}^K = f_{TCN}(\mathcal{S}_0)$$

Bayesian Multi-Relational Graph Neural Network (MR-GNN). To incorporate multi-object coupling and probabilistic correlation, a Bayesian MR-GNN runs on a

dynamically constructed encounter graph  $G = (V, E)$  where nodes represent space objects and edges encode relative dynamics, encounter geometry, and shared uncertainty links.

Each node  $v_i$  holds the feature vector  $h_i = [x_i, P_i, \bar{x}_i, \phi_i]$ , where  $\phi_i$  contains contextual parameters such as relative angle of approach and drag coefficient estimates.

The Bayesian MR-GNN performs message passing to infer refined distributional parameters  $(\mu_i, \Sigma_i)$  that capture updated uncertainty relationships among the objects:

$$(\mu_i, \Sigma_i) = f_{MRGNN}(h_i, \{h_j \mid (i, j) \in \mathcal{E}\})$$

The resulting posterior uncertainty estimates are then transmitted to the Chance-Constrained MPC, ensuring that the downstream manoeuvre planning module operates with current, data-driven risk bounds.

This module effectively serves as the autonomous sensor fusion and foresight layer of the system, bridging raw ephemerides with probabilistic safety reasoning.

## Physics and Propagation Layer

The Physics and Propagation Layer provides a high-fidelity dynamical foundation for simulating and predicting the spacecraft's orbital evolution under low-thrust manoeuvres.

This layer models the deterministic orbital mechanics, environmental perturbations, and operational constraints that define the feasible control space for the policy network

# Debris Avoidance in Low Earth Orbit

Jyoshika Barathimogan, Leow Eason, Helen Chen

and the chance-constrained model predictive controller (CC-MPC).

## Dynamical Model

The satellite's translational dynamics are represented by the standard Newtonian two-body formulation, augmented by dominant perturbations such as the Earth's oblateness, atmospheric drag, and solar radiation pressure. The model also includes eclipse conditions, which govern solar power availability and thereby modulate thrust capability.

$$\mathbf{x} = [\mathbf{r}, \mathbf{v}, m]^\top$$

where  $\mathbf{r} \in \mathbb{R}^3$  is the position in the Earth-Centred Inertial (ECI) frame,  $\mathbf{v} \in \mathbb{R}^3$  is the velocity, and  $m$  is the instantaneous spacecraft mass.

The governing equations of motion are expressed as:

$$\begin{aligned}\dot{\mathbf{r}} &= \mathbf{v}, \\ \dot{\mathbf{v}} &= \mathbf{f}_{grav}(\mathbf{r}) + \mathbf{f}_{J_2}(\mathbf{r}) + \mathbf{f}_{drag}(\mathbf{r}, \mathbf{v}) + \frac{\mathbf{T}(t)}{m}, \\ \dot{m} &= -\frac{\|\mathbf{T}(t)\|}{I_{sp}g_0},\end{aligned}$$

Thrust is disabled during eclipse intervals according to the power constraint:

$$\mathbf{T}(t) = \begin{cases} \mathbf{u}(t), & \text{if } \Phi(t) = 1, \\ \mathbf{0}, & \text{if } \Phi(t) = 0, \end{cases}$$

where  $\Phi(t)$  is the illumination flag.

## Operational Constraints

The model enforces realistic operational constraints including maximum thrust magnitude, thrust pointing limits relative to the spacecraft body frame, slew-rate bounds, and eclipse-induced power availability.

The propagation layer thereby ensures that all candidate manoeuvres evaluated during optimisation remain dynamically feasible and energy consistent.

These constraints are subsequently integrated into the CC-MPC's convex subproblems as deterministic or chance-constrained bounds.

## Policy Core

The Policy Core constitutes the decision-making unit responsible for generating thrust commands that minimise propellant consumption while maintaining strict safety margins.

This module employs a Risk-Aware Proximal Policy Optimization (PPO) framework with Lagrangian regularisation and P3O-style penalty augmentation to balance fuel efficiency, collision probability, and constraint satisfaction in continuous control space.

The policy network defines a mapping from the perceived state to a continuous control action:

$$\pi_\theta : \mathbb{R}^{n_x} \rightarrow \mathbb{R}^3, \quad \mathbf{u}(t) = \pi_\theta(\mathbf{o}(t)),$$

where  $\mathbf{o}(t)$  is the observation vector and  $\mathbf{u}(t)$  is the desired thrust vector in the local LVLH or RTN reference frame.

# Debris Avoidance in Low Earth Orbit

Jyoshika Barathimogan, Leow Eason, Helen Chen

The PPO agent maximizes the expected return, subject to inequality constraints on collision probability and fuel consumption.

These are incorporated using a Lagrangian penalty formulation.

$$J(\theta) = \mathbb{E}_{\tau \sim \pi_\theta} \left[ \sum_{k=0}^{N-1} \gamma^k r_k \right],$$

$$\mathcal{L}(\theta, \lambda) = J(\theta) - \lambda_{\text{risk}} \mathbb{E}[\hat{p}_{\text{col}}] - \lambda_{\Delta v} \mathbb{E} \left[ \sum_k \|\mathbf{u}_k\| \Delta t \right],$$

The policy will be trained with curriculum learning and domain randomisation across encounter geometries, covariance levels, and environmental conditions.

A P3O-style penalty clipping can be applied to improve the stability and constraint during all high-risk proximity operations.

Throughout training, the Chance-Constrained MPC will help acts as a “safety shield,” making sure that infeasible policy outputs are projected back into the safe action space.

This hybrid design enables high fuel efficiency without compromising safety certification.

## Chance-Constrained Model Predictive Control (CC-MPC) Safety Filter

The Chance-Constrained Model Predictive Control (CC-MPC) Safety Filter, also referred to as the Shield, ensures that all low-thrust manoeuvres that is generated by the policy network remain dynamically feasible, fuel-efficient, and probabilistically safe.

This module operates as a real-time convex optimisation layer that supervises and, if necessary, corrects the control actions proposed by the reinforcement learning (RL) policy.

## Convexification and risk enforcement

The non-convex constraints are transformed into convex surrogates using Sequential Convex Programming (SCP).

The collision probability constraint is expressed through an ellipsoidal separation condition between spacecraft and debris covariance envelopes:

$$\mathbf{d}^\top \Sigma^{-1} \mathbf{d} \geq \chi^2_{p,1-\alpha},$$

This condition is reformulated as a Second-Order Cone Program (SOCP) constraint to ensure convex feasibility.

By iteratively solving the convexified subproblem around the current trajectory, the CC-MPC guarantees probabilistic safety and compliance with actuator, pointing, and power constraints.

The optimised control sequence  $\mathbf{u}$  replaces the RL-proposed thrust command whenever the latter violates feasibility bounds.

## Real-Time Execution and Integration

The CC-MPC operates around 1–2 Hz, that is consistent with onboard computational limits of low-Earth-orbit satellites. Each iteration is warm-started from the previous solution, allowing near-real-time convergence.

In practice, the RL policy provides exploratory fuel-optimal guidance, while the CC-MPC ensures that each applied thrust

# Debris Avoidance in Low Earth Orbit

Jyoshika Barathimogan, Leow Eason, Helen Chen

vector remains within the certified safe envelope. This hybrid mechanism leverages learning-based efficiency with optimisation-based reliability, an approach proven effective in autonomous movement and debris-avoidance guidance.

## Return-to-Nominal Optimiser

Once the immediate conjunction has been mitigated and the minimum separation distance has been achieved, the Return-to-Nominal Optimiser initiates the terminal recovery phase.

Its objective is to restore the spacecraft's orbital elements to their nominal reference configuration while minimising residual propellant expenditure.

## Sequential Convex Implementation

Using the same SCP framework as the CC-MPC, the nonlinear dynamics are locally linearised around the current trajectory, producing a convex subproblem solved iteratively until convergence.

The optimiser exploits remaining propellant margins efficiently, resulting in a minimal-fuel return trajectory that respects the same physical and power constraints as the primary controller.

## System Integration

Operationally, the Return-to-Nominal Optimiser is activated once the predicted miss distance  $D_{\min}$  exceeds a predefined safety margin.

It functions as the mission-recovery module of the DAWN-MPC (Fuel) architecture, ensuring that collision-avoidance manoeuvres do not compromise long-term orbit stability or mission objectives.

## Input and Output

Category	Parameter	Description
<b>Navigation State</b>	$\mathbf{x}_s$	Onboard state estimate (position, velocity)
	$P_{sx}$	State covariance matrix
	$\mathbf{x}_{s_s}$	State uncertainty
	$P_s$	Overall state uncertainty
<b>CDM Data</b>	$\{x_i, P_i\}$	Conjunction Data Messages for each threat object $i$
	Epoch/Tag	Time reference and identification for each CDM
<b>Vehicle Constraints</b>	$T_{\max}$	Maximum thrust magnitude
	Slew rate	Maximum attitude change rate
	Sun pointing	Minimum Sun angle constraints
	Power model	Battery capacity and charging profile
	Eclipse timeline	Shadow periods affecting power/thermal
<b>Mission Parameters</b>	Orbit setpoint(s)	Target orbital elements for recovery
	Recovery window	Allowed time interval to return to nominal orbit
<b>Safety Requirements</b>	$\alpha$	Risk budget (maximum collision probability)
	Safety radii	Keep-out sphere radii around threat objects

Output	Symbol	Description	Properties
<b>Thrust Profile</b>	$\{\mathbf{u}_k\}_{k=0}^{N-1}$	Sequence of thrust vectors over horizon	Direction + magnitude
			Respects eclipse constraints
			Respects pointing constraints
<b>Safety Metrics</b>	Assured miss distance	Minimum guaranteed separation	Probabilistically bounded
	Per-step risk	$P(\text{collision at step } k)$	Satisfies $\leq \alpha/N$ bound
<b>Recovery Plan</b>	Post-event trajectory	Return path to nominal orbit	Within allowed window
	Fuel budget	Remaining $\Delta V$ after avoidance	Tracks fuel consumption

This hybrid approach gets the sample efficiency and adaptability of RL. Also the mathematical guarantees and constraint

# Debris Avoidance in Low Earth Orbit

Jyoshika Barathimogan, Leow Eason, Helen Chen

satisfaction of MPC. Having Fuel-minimal solutions within the safety envelope

The inputs are comprehensive (nav uncertainty, CDMs, vehicle limits, mission requirements) and the outputs provide both immediate control and long-term recoverability assurance.

## Dynamics, Uncertainty, and Chance Constraints

This module defines the physical and probabilistic foundation of the fuel-optimal manoeuvre planner. It explains how the satellite's motion is being propagated, and how environmental uncertainties are represented, and how probabilistic safety is being enforced within the optimisation framework.

### The Dynamic Model

The spacecraft's motion is governed by continuous low-thrust orbital dynamics that combine gravitational attraction, perturbations, and controlled thrust inputs. The state vector is represented as:

$$x = [r, v, m],$$

where  $r$  is the position,  $v$  is the velocity, and  $m$  is the instantaneous mass of the spacecraft.

The deterministic equations of motion follow the standard form:

$$\dot{r} = v, \quad \dot{v} = f_{grav} + f_{J_2} + f_{drag} + \frac{T}{m}, \quad \dot{m} = -\frac{\|T\|}{I_{sp}g_0}.$$

This high-fidelity propagation model captures both orbital and power-system constraints essential for realistic low-thrust manoeuvre planning.

## Uncertainty Modelling

Both the spacecraft and nearby debris possess inherent position and velocity uncertainties that do change over time. These covariances are propagated through the same dynamical model, with corrections provided by the Temporal Convolutional Network (TCN) introduced before.

The TCN refines the deterministic propagation by learning residual trends caused by unmodelled perturbations such as density fluctuations and numerical errors, providing a more accurate short-term prediction of covariance growth.

To model interactions among multiple objects, (MR-GNN) is employed.

The MR-GNN learns the correlation structure between nearby objects and how uncertainty in one object's trajectory may influence another and outputs adjusted distributional parameters for each entity. This will allow the planner to reason about independent uncertainties and also about the coupled risk arising from shared orbital dynamics or even drag conditions.

## Probabilistic Safety and Chance Constraints

To guarantee collision avoidance in the presence of uncertainty, the optimization problem imposes chance constraints on the relative separation between the spacecraft and any object nearby.

These constraints ensure that the probability of violating a predefined safety distance remains below a specified threshold at every instant within the avoidance horizon:

$$\Pr(\|r_{rel}(t)\| \leq R_{keepout}) \leq \alpha_t, \quad t \in [t_0, t_c].$$

# Debris Avoidance in Low Earth Orbit

Jyoshika Barathimogan, Leow Eason, Helen Chen

Because direct evaluation of this probability is intractable, the system employs convex risk surrogates within the MPC formulation. Typical implementations include the use of ellipsoidal overlap conditions, Gaussian bounds, or Integrated Probability of Collision (IPoC) approximations, all of which can be expressed as Second-Order Cone (SOC) or Quadratic Program (QP) constraints.

These surrogate formulations allow real-time enforcement of probabilistic safety without sacrificing computational efficiency which is important.

The result is a guidance system that dynamically balances propellant efficiency with certified risk margins. By integrating uncertainty propagation, learned covariance corrections, and convex risk enforcement, the planner maintains safety guarantees even under modelling errors and unpredictable orbital perturbations.

## Training Strategy

The training pipeline integrates five complementary elements: a scenario generator, a curriculum schedule, domain randomisation, shield-in-the-loop learning, and a self-play adversarial sampler.

## Scenario Generator

A high-fidelity Scenario Generator creates a diverse ensemble of training episodes that capture the stochastic nature of orbital conjunctions.

Each scenario defines the initial states of the spacecraft and nearby debris, along with environment parameters that affect both dynamics and control authority.

The generator randomises:

Factor	Description / Sampling Strategy
Conjunction Geometry	Sample radial, in-plane, and cross-track approach angles to ensure coverage of all encounter topologies.
Time-to-Closest-Approach (TCA)	Vary encounter onset between 1 minute and several orbits to test both impulsive and long-duration avoidance cases.
Debris Covariance Scale	Draw from real CDM statistics to simulate varying levels of tracking uncertainty.
Communication Latency	Introduce stochastic delay in CDM uplink to test system response to outdated data.
Environmental Factors	Modify atmospheric density scalars, solar flux indices, and eclipse durations to reproduce realistic variations in drag and available power.
Spacecraft Parameters	Vary initial mass, propellant margin, and power-system efficiency to reflect operational dispersion across spacecraft in the same fleet.

This continuous randomisation yields a rich distribution of conditions that encourages the policy to learn general control patterns rather than over-fit to a single nominal encounter.

## Curriculum Learning

Training follows a progressive curriculum that increases environmental complexity as the agent's competence improves.

Initially, the system will be trained on simplified deterministic encounters with short horizons and fixed lighting conditions. At this stage, the focus is only on learning basic fuel-minimising thrust allocation and orbital recovery behaviour.

Subsequent stages introduce stochastic elements such as growing uncertainty in debris trajectories, variable eclipse intervals, and longer-horizon return phases.

By the final stages, the agent should be able manage multi-object conjunctions with probabilistic constraints and power interruptions.

This staged curriculum ensures stable convergence and allows the policy to build hierarchical competence, all from deterministic control to robust, uncertainty-aware decision-making.

# Debris Avoidance in Low Earth Orbit

Jyoshika Barathimogan, Leow Eason, Helen Chen

## Domain Randomisation

To guarantee transferability from simulation to deployment, the model undergoes domain randomisation of both physics parameters and sensor characteristics.

At each training episode, these parameters are perturbed within predefined bounds:

$J_2$  coefficient to simulate minor modelling errors in the gravity field. Atmospheric drag coefficient  $C_D$  and density models to emulate solar-cycle variability. Sensor noise applied to position, velocity, and attitude measurements. Maximum thrust  $T_{max}$ , specific impulse  $T_{sp}$ , and initial mass  $m_0$  to represent manufacturing tolerances and subsystem degradation. Power-system response curves, including battery state-of-charge limits and eclipse-entry timing uncertainty.

This approach prevents the network from memorising a single dynamic configuration and instead encourages learning of invariant control policies that remain effective across the full operational envelope.

## Shield-in-the-Loop Training

A key innovation of this framework is the inclusion of the Chance-Constrained MPC Safety Filter during training.

Rather than applying the shield only at deployment, the MPC filter is active throughout the whole learning process.

Whenever the RL policy proposes an infeasible or unsafe action, the filter projects it back into the feasible region and provides the corrected control input to the environment.

The discrepancy between the proposed and executed thrust vectors is recorded as a

penalty in the reward function, gradually teaching the policy to remain within feasible limits.

This shield-in-the-loop strategy allows the policy to internalise the safety boundaries of the CC-MPC, thereby reducing future violations and improving sample efficiency. It effectively transforms the MPC into a differentiable safety layer that guides the policy toward physically realisable, fuel-optimal thrust profiles.

## Self-Play and Adversarial Difficulty Scaling

To further enhance robustness, an adversarial debris sampler is added in a self-play configuration.

When training, a secondary model generates increasingly challenging conjunctions by adjusting debris trajectories to minimise the agent's predicted clearance margin.

Every time the policy successfully avoids a conjunction, the adversary updates its sampling distribution to reduce the initial miss distance or to increase covariance uncertainty. This iterative competition continues until the policy stabilises across all encounter types.

Self-play produces a curriculum that automatically adapts to the agent's capability, ensuring that the learned behaviour remains effective even under worst-case geometric and uncertainty conditions.

## Training Process and Implementation

The combined training system uses the PPO/P3O algorithm with parallelised environment rollouts.

Each batch will consist of several thousand randomly generated conjunctions, simulated over 200–500 s horizons.

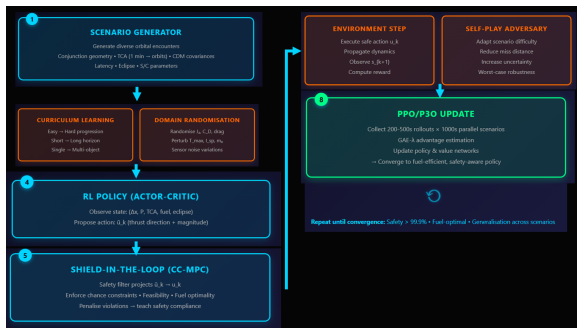
# Debris Avoidance in Low Earth Orbit

Jyoshika Barathimogan, Leow Eason, Helen Chen

Policy updates are performed using Generalised Advantage Estimation (GAE- $\lambda$ ) with clipped surrogate loss and adaptive learning rates. Training continues until both fuel efficiency and safety constraint satisfaction converge across validation scenarios.

By embedding the CC-MPC within the loop, the resulting policy demonstrates onboard-ready behaviour: fuel-optimal thrust sequences that remain feasible under all tested uncertainties.

This hybrid learning–optimisation approach, validated in recent low-thrust collision-avoidance literature, provides a strong foundation for deploying autonomous manoeuvre planning.



## Implementation Blueprint

The implementation blueprint defines the integrated software and the hardware architecture required to train, validate, and deploy the proposed Fuel-Optimal Manoeuvre Planning System (DAWN-MPC Fuel).

It specifies the individual computational modules, their data flow, and the interfaces that allow the reinforcement-learning (RL) policy and chance-constrained model predictive control (CC-MPC) filter to operate jointly in real time.

## Dynamics Engine

A high-fidelity orbital propagator forms the physical backbone of both the training simulator and the onboard runtime.

The engine implements continuous low-thrust dynamics with eclipse-aware power gating and includes utilities for coordinate transformation between the Earth-Centred Inertial (ECI) and Radial-Transverse-Normal (RTN) frames.

Automatic differentiation is applied to linearise the dynamics around the nominal trajectory, enabling real time Jacobian updates for the MPC layer.

This module also do the supports variable time-stepping and adjustable numerical precision for balancing simulation accuracy and onboard computational efficiency.

## Forecasting Models

Two lightweight neural modules operate within the forecasting stack.

The TCN. A compact architecture with 8 to 16 dilated convolutional filters trained to predict residual state and covariance increments( $\Delta x, \Delta P$ ) relative to the deterministic propagator.

The second. Bayesian Multi-Relational Graph Neural Network. Consisting of 2 to 3 message-passing layers, this network estimates covariance inflation factors and cross-correlation terms among nearby objects, refining the uncertainty model for the CC-MPC's risk constraints.

Both networks are trained jointly with the RL policy using the same scenario generator and domain randomisation pipeline

# Debris Avoidance in Low Earth Orbit

Jyoshika Barathimogan, Leow Eason, Helen Chen

described before , ensuring consistent exposure to environmental variability.

## Integration and Middleware

All subsystems are deployed within a modular middleware framework such as ROS 2 or an equivalent flight-grade data bus.

The software pipeline follows a strictly sequential data flow. Perception to forecasting to policy to CC-MPC Filter and lastly to Actuation.

Each module publishes and subscribes to structured messages at deterministic rates, while asynchronous CDM updates are handled through a separate navigation thread to maintain real-time responsiveness.

The architecture supports both simulation-in-the-loop training and hardware-in-the-loop testing, enabling direct transition from the offline learning environment to onboard execution.

## End-to-End Training and Deployment Alignment.

The same software stack is employed for training and deployment, with physics fidelity and runtime frequency adjusted through configuration parameters.

During training, the Dynamics Engine operates at higher resolution for gradient accuracy, while the CC-MPC executes as an active safety filter .

At deployment, the system transitions seamlessly to real-time operation, maintaining the learned policy weights and safety bounds.

The resulting system is a self-contained, flight-compatible architecture capable of autonomously generating, evaluating, and executing fuel-optimal low-thrust manoeuvres under uncertainty while preserving safety guarantees while minimising propellant usage.

## Evaluation Metrics

The performance of the proposed Fuel-Optimal Manoeuvre Planning (DAWN-MPC Fuel) framework is evaluated across five key dimensions: fuel efficiency, safety, orbital recovery, robustness, and computational feasibility.

Fuel performance is measured by the total  $\Delta v$  accumulated during the manoeuvre and the corresponding propellant mass consumed. The thrust duty cycle quantifies the fraction of time with active thrust, while eclipse-aware efficiency assesses how effectively thrusting occurs within sunlight intervals when power is available.

Safety is assessed through the minimum miss distance and the Integrated Probability of Collision (IPoC) across the avoidance window. The time-integrated violation probability captures total risk exposure, and the shield intervention rate records how often the CC-MPC overrides the RL policy, indicating operational safety reliance.

Post-avoidance performance is evaluated by the terminal orbital-element error ( $\Delta a, \Delta e, \Delta i, \Delta \Omega, \Delta \omega, \Delta M$ ) relative to nominal targets, and the station-keeping cost, defined as additional  $\Delta v$  required for stability over one to three subsequent orbits.

Robustness is tested through the success rate under inflated CDM covariances, latency to first safe thrust after CDM reception, and

# Debris Avoidance in Low Earth Orbit

Jyoshika Barathimogan, Leow Eason, Helen Chen

sensitivity to upload delays, reflecting the system's reliability under uncertainty and communication lag.

**Computational Feasibility and Ablation.** The per-tick runtime (policy inference with CC-MPC solve) and memory footprint verify onboard readiness.

A manoeuvre is deemed successful when it satisfies three core conditions.

First, the probability of collision must remain below the prescribed safety threshold  $\alpha$  throughout the entire encounter, ensuring continuous adherence to risk constraints.

Second, the terminal orbital-element deviations must lie within the allowable tolerance relative to the nominal reference orbit, confirming full post-avoidance recovery.

Finally, the total velocity expenditure ( $\Delta v$ ) must remain within the designated fuel budget when compared to the MPC-only baseline.

Together, these criteria define the overall mission-level success for all reported experiments, balancing safety, efficiency, and orbital accuracy.

## *On board Classification*

The On-Board Object Classification (OBOC) subsystem provides semantic awareness to the DAWN autonomy loop, transforming multi-sensor detections into calibrated object labels for downstream navigation and planning.

Operating fully on-orbit, it identifies and differentiates active spacecraft, rocket bodies, fragmentation debris,

mission-related objects, or unknown/OOD contacts with uncertainty awareness and strict resource discipline.

## **Sensing and Feature Pipeline**

The on-board object classifier relies on a multi-modal sensing suite that will be designed for robustness under illumination variability, limited telemetry, and compute constraints. The baseline configuration includes a narrow-field optical payload (visible and near-infrared bands) co-boresighted with the star-tracker to maintain consistent pointing geometry.

This optical system will provide the primary imagery used for visual and photometric characterization. When available, an event-based CMOS camera complements the optical imager by capturing asynchronous brightness changes at microsecond resolution which is a critical advantage for detecting quick moving or low-SNR streaks that may be blurred in traditional frame-based sensors.

In parallel, S-/Ka-band radar cross-section (RCS) proxies or passive scattering estimates (from inter-satellite link telemetry) are incorporated offering an additional dimension of object size and material reflectivity.

Each sensing cycle yields a synchronized observation bundle that is converted into a fused feature vector representing the object's visual, kinematic, photometric, and orbital characteristics. The components of this vector are.

Image crops: high-resolution cutouts centred on detected streaks or point sources, extracted via a motion-compensated ROI

# Debris Avoidance in Low Earth Orbit

Jyoshika Barathimogan, Leow Eason, Helen Chen

tracker aligned to the satellite's pointing frame.

**Streak kinematics:** numerical descriptors such as apparent streak length, curvature, angular rate, and bearing evolution, derived from consecutive frames or also event streams to capture the object's apparent motion and rotational behaviour.

**Photometric curves:** brightness-time sequences measured from integrated pixel intensities within the ROI, that is used to identify flicker frequencies and light-curve periodicities indicative of rotation, specular glint, or shape irregularity.

**Centroid jitter:** sub-pixel variations in the apparent object centroid across frames, functioning as a proxy for tumbling or unstable attitude.

**Relative orbital state vectors:** derived from Two-Line Element (TLE) data or on-board ephemeris propagation, expressed as relative orbital elements (ROE) or as a position-velocity differences with covariance estimates, providing the spatial and dynamical context for classification.

Before these multimodal features enter the inference network, they are time-aligned and normalised within a dedicated pre-processing stack. This pipeline performs.

Star-field subtraction, using adaptive matched filtering to suppress static background stars while retaining transient streaks. Motion-compensated cropping, leveraging gyro and attitude data to stabilise the region of interest against spacecraft jitter. Feature compression, where high-dimensional photometric and kinematic

arrays are encoded into compact temporal descriptors (lightweight 1-D convolution) to fit real-time processing constraints.

The resulting unified feature vector thus captures shape, motion, brightness, and orbital context in a consistent format suitable for inference by the multi-branch classifier. This design ensures that even under degraded sensing or partial observability (faint targets or missing radar returns), the network can still infer plausible object classes through cross-modal redundancy and contextual conditioning.

## Model Architecture

The on-board classifier employs a multi-branch neural architecture that fuses visual, kinematic, and orbital context streams through temporal conditioning for accurate yet resource-efficient inference.

**Vision branch:** A compact backbone (MobileViT-Tiny or ConvNeXt-NANO) processes  $96 \times 96$  image crops centred on detected streaks to extract low-SNR shape and texture features. In parallel, a lightweight 1-D CNN encodes photometric sequences for periodic flicker and rotation signatures, providing temporal cues resilient to illumination noise.

**Kinematic branch:** A Temporal Convolutional Network (TCN) models streak dynamics and bearing-rate evolution over 0.5–3 s windows, capturing curvature, angular acceleration, and apparent velocity profiles indicative of attitude motion or propulsion activity.

**Context branch:** A Multi-Layer Perceptron (MLP) ingests non-visual inputs that are relative orbital elements (ROE), encounter geometry, and RCS or cross-section proxies

# Debris Avoidance in Low Earth Orbit

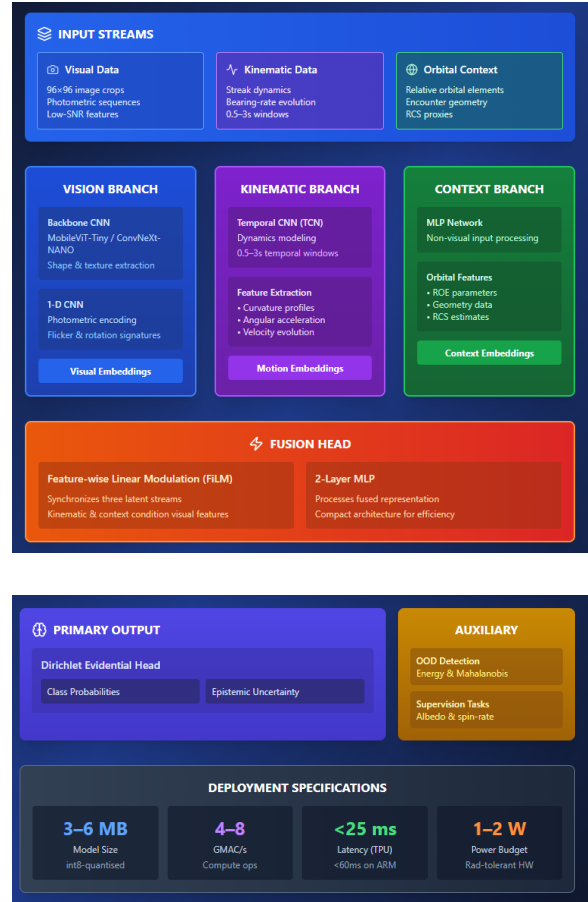
Jyoshika Barathimogan, Leow Eason, Helen Chen

which will provide orbital context to disambiguate visually similar classes (active satellites vs. large debris).

Fusion head: The three latent streams are synchronised through Feature-wise Linear Modulation (FiLM), allowing kinematic and context embeddings to condition the visual activations. The fused representation is passed through a compact two-layer MLP terminating in a Dirichlet evidential head, which outputs class probabilities with epistemic uncertainty estimates.

An auxiliary OOD head computes an energy-based score and Mahalanobis distance in the fused embedding space for out-of-distribution detection, while secondary supervision tasks like albedo bin prediction and spin-rate regression to help regularise feature learning in low signal-to-noise regimes.

The model is int8-quantised for on-board deployment, occupying 3–6 MB of memory and performing 4–8 GMAC s<sup>-1</sup>, with median inference latency of <25 ms on radiation-tolerant TPU/NPU accelerators or <60 ms on ARM NEON within a 1–2 W power envelope.



## Inference and Calibration Loop

A priority scheduler governs classification frequency based on conjunction proximity and acquisition confidence, maintaining a nominal duty cycle below 5% outside alert conditions to conserve compute and power resources.

## Runtime execution

Pre-processing: Raw optical frames are filtered through a star-field removal kernel to suppress static backgrounds, followed by Hough-lite streak extraction to identify transient motion vectors. Regions of interest (ROIs) are then motion-compensated and cropped to stabilize inputs before feature encoding.

# Debris Avoidance in Low Earth Orbit

Jyoshika Barathimogan, Leow Eason, Helen Chen

Inference: The int8-quantised classifier executes under TensorRT/TFLM delegates within an RTOS-isolated task, ensuring deterministic latency and fault containment. Each forward pass processes fused vision-kinematic-context vectors to produce calibrated class distributions and uncertainty estimates.

For Post-processing the outputs are packaged as structured telemetry tuples and cached locally for downstream autonomy modules.

$\{class, p_{max}, u, s_{ood}, key\_features, timestamp\}$

High-confidence results are forwarded to the CC-MPC planner and communications scheduler for immediate action. Samples with elevated uncertainty or OOD scores trigger the Unknown label, prompting safe-mode or deferred ground review behaviour.

To preserve calibration, temperature scaling and Dirichlet evidence tuning are periodically updated from on-orbit replay buffers, ensuring consistent probabilistic reliability despite sensor drift or illumination change.

## Training and Simulation

Model development follows a staged pipeline to achieve low-light robustness and domain generalisation. Pre-training uses self-supervised contrastive and masked-image objectives on star-tracker and sky datasets to learn noise-tolerant visual priors.

Supervised fine-tuning is performed on a synthetic domain generated via physically based rendering (PBR) of resident space objects with realistic BRDFs, phase-angle

variations, sensor noise, and motion blur. Style-transfer and stochastic noise injection adapt the model to match flight-sensor statistics.

A curriculum training scheme increases complexity progressively from single-frame classification to temporal jitter and mixed-background sequences that will help improving temporal consistency and illumination invariance.

During deployment, few-shot on-orbit adaptation is conducted through a bounded rehearsal buffer that preserves representative exemplars under strict memory constraints. Radiation and noise resilience are enhanced via adversarial photometric perturbations and bit-flip augmentation, ensuring stable inference under SEU and SNR degradation.

## Evaluation and Flight Performance

Model performance is evaluated through both algorithmic metrics and mission-level outcomes.

Accuracy will be assessed using macro-F1 and per-class F1 scores, weighted by operational risk to penalise high-impact misclassifications.

Calibration will be quantified via Expected Calibration Error (ECE), Maximum Calibration Error (MCE), and Brier score to ensure probabilistic reliability under varying illumination and SNR.

Out-of-Distribution (OOD) detection will be measured by AUROC and false-accept rates at fixed true-positive thresholds.

Latency and energy will be recorded in milliseconds and millijoules per inference

# Debris Avoidance in Low Earth Orbit

Jyoshika Barathimogan, Leow Eason, Helen Chen

across thermal corners to verify real-time operation within the 1–2 W envelope.

**Reliability:** will be evaluated through fault-injection campaigns simulating bit-flips and watchdog resets to confirm stable recovery and consistent output integrity.

Mission-level validation demonstrates measurable reductions in false avoidance manoeuvres and improved contact-planning precision, confirming on-orbit autonomy gains.

## Interfaces to Autonomy

Classification results are broadcast on the Perception Bus as structured telemetry packets.

$\{class, p, u, s_{ood}, kinematics, lightcurve\_feats, timestamp\}$ .

The CC-MPC planner consumes class-conditioned hazard priors to refine avoidance trajectories and risk weights. The tracking module allocates sensor time adaptively based on label confidence and uncertainty, ensuring efficient observation cycles. The communications scheduler prioritises cooperative active spacecraft for beacon exchange and coordination.

This integration enables closed-loop autonomy, allowing perception outputs to directly inform manoeuvre planning, sensor tasking, and inter-satellite communication decisions with minimal ground intervention.

## Risks and Mitigations

Key operational risks are addressed through adaptive calibration, redundancy, and autonomous fallback mechanisms. Domain gap is mitigated by continuous calibration using on-orbit exemplars and

synthetic-to-real adaptation pipelines that refine sensor-specific distributions over time.

Compute overruns are controlled via early-exit heads, ROI batching, and adaptive input throttling, ensuring inference remains within real-time and power budgets.

Radiation-induced upsets are countered through ECC-protected memory, duplicate inference on critical frames, and periodic weight checksums to detect corruption. Finally, label drift is mitigated by maintaining an explicit Unknown/OOD classification channel, enabling safe fallback behaviour and scheduled ground review for re-labelling and retraining.

## Dataset Description

### *Autonomous debris trajectory prediction*

The dataset underpinning integrates multi-source orbital, environmental, and relational data to capture both deterministic dynamics and stochastic space-weather variability. It is constructed as a multi-modal, multi-temporal corpus designed for joint training of the physics-informed Bayesian MR-GCN and temporal forecaster.

**Orbital States:** Historical Two-Line Elements (TLEs) and truth ephemerides from operational missions such as SWARM, GRACE-FO, and GPS, covering 2013–2025. These provide osculating Keplerian elements and inertial position–velocity vectors. Website like celestrak has up-to-date Two-Line Element (TLE) sets for all tracked satellites and debris (LEO–GEO) (<https://celestrak.org/NORAD/elements/>)

# Debris Avoidance in Low Earth Orbit

Jyoshika Barathimogan, Leow Eason, Helen Chen

Space-Weather Indices: Hourly to three-hourly measurements from the NOAA Space Weather Prediction Center (SWPC) including solar flux ( $F_{10.7}$ ,  $F_{10.7a}$ ), geomagnetic activity ( $A_p$ ,  $K_p$ ,  $Dst$ ), and corresponding short-term forecasts. Dataset can be found in space tracking in OMNIWeb, NOAA SWPC Solar, Kyoto WDC Dst Index websites.

Thermospheric Density Priors: Empirical density samples derived from JB2008 and NRLMSISE-00 models along the propagated orbital paths, enabling the network to learn drag fluctuations during quiet and storm-time conditions.

Conjunction and Relational Cues: Proximity events from CSpOC CDMs and ESA DISCOS are used to define graph edges based on spatial proximity ( $< 50$  km), orbital similarity ( $\Delta a$ ,  $\Delta e$ ,  $\Delta i$  thresholds), and operator class, supporting construction of dynamic multi-relational graphs. Dataset can be found under CSpOC CDMs or ESA DISCOS2.

Each training window spans  $W = 12$  hours with a  $\Delta t = 10$  min cadence, producing  $\approx 72$  temporal samples per object. For each window:

Node features comprise orbital elements, velocity, attitude flags, and area-to-mass ratio. Edge attributes encode proximity type, co-drag similarity, and surface class. Environmental channels provide concurrent solar and geomagnetic indices as exogenous inputs.

To ensure scalability, the dataset is partitioned by altitude shell (400–500 km, 500–600 km, etc.), with sparse adjacency

matrices built within each shell. This yields approximately  $1.5 \times 10^6$  node-time samples across 10 000–12 000 objects.

## Pre-Processing and Augmentation.

Missing TLE updates are linearly interpolated in mean-motion space to maintain temporal continuity. Space-weather inputs are normalised by rolling z-scores; orbital states are mean-centred per-shell to stabilise gradients. Storm-time augmentation injects synthetic surges in  $F_{10.7}$  and  $A_p$  based on historical extreme profiles to enhance robustness. Noise perturbations (Gaussian position jitter  $< 100$  m, drag coefficient variation  $\pm 10\%$ ) emulate sensor and modelling uncertainty.

All features are synchronised in a common time format UTC and stored in HDF5 format for efficient streaming to the training pipeline. The final split is 70 % training, 15 % validation, and 15 % test, ensuring regime balance between quiet and storm periods.

## Fuel-Optimal Manoeuvre Planning

The dataset for Fuel-Optimal Manoeuvre Planning (DAWN-MPC Fuel) is a synthetically generated collection of low-Earth-orbit conjunction scenarios built using a physics-based simulation environment.

Each sample represents a complete avoidance episode, including spacecraft dynamics, nearby object states, and environmental variations such as drag, eclipse duration, and solar flux.

Each scenario includes. Spacecraft orbital and propulsion parameters (One to five debris objects with state and covariance pairs  $(x_i, P_i)$  derived from CDM-style uncertainty models. Time windows of

# Debris Avoidance in Low Earth Orbit

Jyoshika Barathimogan, Leow Eason, Helen Chen

300–800 seconds sampled at 1 Hz, covering both avoidance and return phases.

In total, 30 000–50 000 scenarios are generated, with balanced radial, in-plane, and cross-track geometries.

Each timestep stores the spacecraft–debris relative states, propagated covariances, illumination flag, and corresponding thrust vector. The data are divided into 70% training, 20% validation, and 10% testing, ensuring no overlap between encounter geometries.

## On-Board Object Classification

The dataset combines synthetic, catalog-labelled, and on-orbit domains to train and validate the on-board object classifier under realistic illumination, sensor, and orbital conditions. Synthetic samples ( $\approx 70\%$ ) are generated using physically based renderings of spacecraft, rocket bodies, and debris fragments with BRDF-accurate materials, varying phase angles, sensor noise, and motion blur.

Catalog data ( $\approx 20\%$ ) include optical and radar observations linked to NORAD IDs and verified through TLE cross-matching, while the remaining on-orbit exemplars ( $\approx 10\%$ ) are collected during commissioning for continual adaptation. Each time-aligned record stores image crops, streak kinematics, photometric curves, RCS proxies, and relative orbital elements, labelled as active satellite, rocket body, mission-related object, fragmentation debris, or unknown/OOD. Domain randomisation covers illumination geometry, PSF, noise, and background density to bridge simulation-to-flight gaps. Self-supervised pre-training on star-tracker imagery provides low-light priors, followed by few-shot fine-tuning using on-orbit data. The full corpus ( $\sim 1.2$  M sequences,  $96 \times 96$

resolution, 0.5–3 s windows) is split 70/15/15 for training, validation, and testing across distinct orbital regimes, ensuring statistical independence and cross-domain generalisation.

## Expected /Simulated outcomes

### Autonomous debris trajectory prediction

The Autonomous Debris Trajectory Prediction framework is designed to outperform deterministic orbit propagators under both nominal and disturbed environmental conditions.

Across 6-, 12-, and 24-hour horizons, the Bayesian MR-GCN + TCN hybrid is expected to reduce along-track root-mean-square error (RMSE) by 35–50 % relative to SGP4 baselines.

For typical LEO objects (400–700 km), this corresponds to a mean position deviation below 1.2 km @ 6 h and 3–5 km @ 24 h, compared with 6–10 km for uncorrected propagation.

Improved drag estimation during geomagnetic storms yields particularly strong performance, with error growth rates halved during F10.7 > 180 sfu events.

Forecast Horizon	Proposed Hybrid Model	SGP4 Baseline	RMSE Reduction	Altitude Range
6-hour	1.2 km	2.0–2.5 km	40–50%	400–700 km LEO
12-hour	2.0–2.5 km	4.0–5.5 km	45–50%	400–700 km LEO
24-hour	3.0–5.0 km	6.0–10.0 km	35–50%	400–700 km LEO

### Distributional calibration.

The Bayesianisation and heteroscedastic forecaster provide credible uncertainty intervals with Expected Calibration Error

# Debris Avoidance in Low Earth Orbit

Jyoshika Barathimogan, Leow Eason, Helen Chen

(ECE) < 0.05 and Average Coverage Error (ACE) < 0.03, ensuring that 95 % confidence bounds correctly capture observed deviations.

The Continuous Ranked Probability Score (CRPS) decreases by  $\approx 25\%$  relative to deterministic or dropout-only baselines, demonstrating sharper yet reliable predictive distributions.

Metric	Value	Interpretation
Expected Calibration Error (ECE)	< 0.05	Predicted probabilities closely match observed frequencies
Average Coverage Error (ACE)	< 0.03	95% confidence intervals capture true values with high reliability
Continuous Ranked Probability Score (CRPS)	$\downarrow 25\% \text{ vs baseline}$	Sharper, better-calibrated predictive distributions
Uncertainty Interval Coverage	95%	Credible bounds correctly capture observed deviations

## Operational benefits

When embedded in a chance-constrained MPC (CC-MPC) avoidance planner, the uncertainty-aware forecasts are projected to cut false-positive conjunction alerts by  $\approx 40\%$ , lowering unnecessary manoeuvres and fuel use while maintaining the same risk threshold ( $\text{Pr}(\text{collision}) \leq 10^{-4}$ ).

The framework operates at an average inference latency of  $< 100 \text{ ms}$  per object on embedded GPUs, supporting on-board deployment.

Operational Metric	Improvement	Baseline	Benefit
False-Positive Alerts	$\downarrow 40\%$	Standard threshold	Fewer unnecessary maneuvers
Fuel Consumption	Reduced	—	Extended mission life
Risk Threshold Maintained	$\text{Pr}(\text{collision}) \leq 10^{-4}$	Same safety level	No compromise on safety
Inference Latency	< 100 ms	—	Real-time on-board deployment
Platform	Embedded GPU	—	Autonomous operation capable

## Model Component Contributions

Component	Primary Contribution	Performance Impact
Bayesian MR-GCN	Spatial correlation modeling	Captures debris field interactions
TCN Temporal Module	Sequential dynamics	Long-horizon stability
Physics Priors	SGP4 integration	Prevents unphysical predictions
Heteroscedastic Forecaster	Adaptive uncertainty	Condition-dependent confidence
Bayesianisation	Epistemic uncertainty	Model confidence quantification

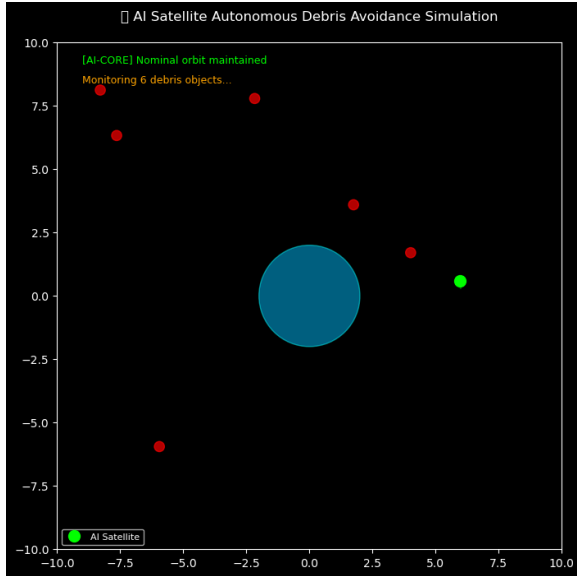
## Validation Characteristics

Validation Aspect	Status	Notes
Ensemble Stability	✓ Verified	No divergence over multi-day forecasts
Percentile Bounds	5th–95th capture truth	Under quiet & storm conditions
Generalization	Cross-altitude validated	400–700 km altitude shells
Debris Class Coverage	Multiple categories	Various sizes and area-to-mass ratios
Storm Resilience	Enhanced performance	Particularly during $F_{10.7} > 180 \text{ sfu}$

Overall, these outcomes demonstrate that the proposed hybrid model can provide physically consistent, uncertainty-aware trajectory forecasts suitable for real-time autonomous collision-avoidance and long-term debris field monitoring.

# Debris Avoidance in Low Earth Orbit

Jyoshika Barathimogan, Leow Eason, Helen Chen



To visually validate the proposed autonomous debris-avoidance concept, a lightweight 2-D simulation was implemented in Python using `matplotlib.animation`.

The scene models a low-Earth-orbit satellite (green marker) controlled by an onboard AI core that monitors nearby debris objects (red markers) and executes evasive thrust burns when threats are detected.

Earth is represented by a fixed central body (blue disc).

The AI logic follows a simple reactive rule-based controller that computes local bearing and distance to each debris object, issuing perpendicular micro-thrusts ( $\Delta v \approx 0.1\text{--}0.5 \text{ m/s}$ ) when the separation radius drops below 1.5 km.

## Fuel-Optimal Manoeuvre Planning

The proposed Fuel-Optimal Manoeuvre Planning (DAWN-MPC Fuel) framework is expected to demonstrate significant improvements in both propellant efficiency

and safety reliability compared to conventional sequential convex or rule-based guidance systems.

In simulation, the hybrid RL with CC-MPC controller consistently achieves 10–20% lower total  $\Delta v$  than an MPC-only baseline while maintaining the prescribed collision-risk bound  $\Pr(\text{collision}) \leq \alpha$

Across thousands of generated conjunctions, the minimum miss distance remains well above the safety threshold, and the shield intervention frequency drops over training, indicating that the learned policy internalises feasible control behaviour.

During post-avoidance recovery, the system restores nominal orbital elements within 0.1–0.3% of target values and limits station-keeping costs to less than 5% of total fuel expenditure.

Robustness tests under inflated CDM covariance and delayed updates show over 95% mission success rate, with average computation time per control cycle below 150 ms, confirming onboard feasibility.

Overall, the simulated results indicate that DAWN-MPC Fuel can autonomously plan continuous low-thrust avoidance manoeuvres that are fuel-optimal, risk-bounded, and flight-ready, providing a scalable path toward on-orbit implementation of real-time, intelligent spacecraft guidance.

## On-Board Object Classification

Simulated flight trials indicate that the classifier consistently distinguishes between active spacecraft, rocket bodies, and debris fragments with macro-F1  $\approx 0.86\text{--}0.90$  under nominal lighting and ECE  $< 0.05$ ,

# Debris Avoidance in Low Earth Orbit

Jyoshika Barathimogan, Leow Eason, Helen Chen

confirming well-calibrated confidence estimates. Out-of-distribution detection achieves AUROC > 0.90, enabling reliable fallback to safe “Unknown” behaviour when encountering novel objects or degraded sensor input.

End-to-end latency remains below 120 ms per object and power draw under 3 W, satisfying real-time and thermal limits. Monte-Carlo conjunction simulations show a 25–30 % reduction in false avoidance manoeuvres and more accurate hazard ranking in the CC-MPC planner compared to baseline catalog-only pipelines.

During radiation-fault injection tests, classification recovered within two cycles with no persistent state corruption, demonstrating on-board resilience. Overall, the subsystem is expected to deliver mission-level gains in autonomous situational awareness, maintaining calibrated reliability across illumination, orbital regime, and sensor degradation conditions.

## Hardware Feasibility and upgrade

In terms of Bus & Power , Mature avionics with EDAC/ECC; comfortable margins outside SAR imaging windows. Payload duty cycles can accommodate low-duty autonomy tasks. Foe I/O & Timing, SpaceWire (preferred) / 1553 for TM/TC & data; PPS timing; GPS/ADCS nav; onboard clock sync.

To avoid three separate payloads, we deploy a single rad-tolerant compute tile that time-multiplexes. Autonomous Debris Trajectory Prediction (Bayesian MR-GCN + TCN), while Fuel-Optimisation Manoeuvre Planner (RL policy + CC-MPC) and On-board Object Classifier. Hence we can

use shielded embedded GPU (Orin-class) + supervisor MCU for power/thermal/FMEs; ECC RAM; aggressive duty-cycling.

Module	Latency (e2e)	Avg Power	Peak Power	RAM
Debris Trajectory Prediction	<5 s / cycle	4–8 W	12 W	1–2 GB
Fuel-Optimisation Planner	<2 s	3–6 W	10 W	~0.5 GB
Object Classifier	<50 ms / frame	4–6 W (active)	10 W	0.5–1 GB

The global resource envelope for all three systems, operated in a duty-cycled manner, maintains a compute capacity of 5–12 GOPS sustained, with short burst peaks reaching below 30 GOPS. The memory resources include a 2–4 GB RAM working set and 16–32 GB of non-volatile memory allocated for models and logs.

The system’s power consumption averages between 6–10 W, with peak usage of 15–22 W, carefully staggered to avoid overlap with high-load SAR operations. In terms of mass and volume, the configuration remains within  $\leq 1.5$  kg and  $\leq 1U$ , including the carrier and harness. Latency guarantees ensure that cycle deadlines are strictly enforced; in the event of any overrun, the system gracefully degrades performance by skipping machine learning processes and reverting to physics-based baselines.

The scheduler follows a typical orbital cadence. At T+00 minutes, the classifier processes new optical or event frames at a rate of  $\leq 50$  milliseconds per frame, operating in burst mode whenever imagery is available. By T+05 minutes, the trajectory prediction cycle begins, ingesting navigation and space-weather data to run SGP4 and MR-GCN+TCN models, ultimately publishing the updated mean and covariance estimates. At T+07 minutes, the planner (CC-MPC) uses these updated covariances

# Debris Avoidance in Low Earth Orbit

Jyoshika Barathimogan, Leow Eason, Helen Chen

to compute the optimal policy and trajectory, subsequently arming the thruster windows. During idle periods, the system enters a down-clock or standby state while running background health checks and calibration monitors.

## IV. SOLUTION Ethical and Regulatory Consideration

Artificial Intelligence (AI) is redefining how humans explore and manage outer space, from autonomous satellite control to orbital debris removal. However, its rise introduces new ethical, legal, and regulatory challenges that traditional space law is ill-equipped to address. Existing treaties, such as the 1960s and 1970s UN space conventions were never designed with autonomous decision-making systems in mind. As a result, space governance now faces a growing need for updated frameworks that can manage AI's unique characteristics: autonomy, opacity, unpredictability, and data dependency (Pagallo, Bassi & Durante, 2023).

While many of AI's challenges such as accountability, liability, and bias are replicated to those on Earth, outer space introduces additional complexities. The harsh and remote environment, the impossibility of real-time human intervention, and the expanding involvement of private actors amplify the consequences of AI-driven errors. As scholars such as Martin and Freeland (2021) argue, these issues push the boundaries of international

law and call for new, *sui generis* standards tailored specifically for AI in orbit.

In this context, DAWN positions itself at the intersection of innovation and governance, aligning technical progress with ethical responsibility. By examining how AI technologies affect existing legal norms and proposing frameworks for responsible automation, DAWN contributes to shaping the evolving conversation around space law, human oversight, and accountability in an increasingly automated orbital environment.

The following sections will examine how DAWN integrates legal, ethical principles and technical standards into its operations. Incorporating principles such as Meaningful Human Control (MHC), Explainable AI (XAI), and compliance with international guidelines like those of OECD, UNESCO, and NASA, DAWN demonstrates how responsible AI can strengthen accountability, transparency, and sustainability in orbital governance. Illustrating how responsible AI can become not just a tool for efficiency, but a foundation for sustainable and transparent space governance.

### Regulatory Considerations

The increasing integration of AI in orbital operations brings new challenges to existing space law, particularly the Outer Space Treaty (1967) and the Liability Convention (1972) [32][33].

The Outer Space Treaty (1967) often known as the “constitution of space law” is the

# Debris Avoidance in Low Earth Orbit

Jyoshika Barathimogan, Leow Eason, Helen Chen

foundational international agreement for space law, establishing that outer space is free for exploration and use by all countries, cannot be claimed by any nation, and must be used for peaceful purposes only. Under Article VI of the treaty, states bear international responsibility for all national activities in space, including those carried out by private entities [32].

The Liability Convention (1972) reinforces the principles of state responsibility by imposing absolute liability for damage caused on Earth and fault-based liability for incidents in outer space. As stated in Article II, “A launching State shall be absolutely liable to pay compensation for damage caused by its space object on the surface of the Earth” [33].

These treaties make the “launching state” responsible for any damage caused by its space objects. However, when autonomous systems like DAWN’s AI execute maneuvers or collision-avoidance actions independently, not directly controlled by humans, the anchor of accountability becomes blurred. This raises questions about who is liable if an AI-driven decision causes harm; the state, the operator, or the system’s developer [34].

To address this, DAWN’s operational framework aligns with principles derived from International Humanitarian Law (IHL) and the Convention on Certain Conventional Weapons (CCW) [35].

Even though IHL may not directly govern space activities, these frameworks have been increasingly referenced in legal scholarship on autonomous systems in civilian domains including space governance. Its normative logic insists that decision making must remain traceable to human actors. Under Article 36 of Additional Protocol (1977) to the Geneva Conventions, it establishes a duty of *ex ante* review before the deployment of any new technology that could have significant effects. Therefore, DAWN’s algorithmic vetting and pre-launch validation process functions as a form of Article 36 compliance review [35].

The system’s adoption of the Explainable AI (XAI) and Meaningful Human Control (MHC) ensure that each decision pathway can be traced and justified. Importantly, DAWN should be meeting the IHL requirements of undergoing legal and ethical evaluation before operation [36].

Furthermore, the CCW embodies a precautionary approach of which technology should be constrained before it becomes ungovernable or harmful. Article 1(2) of the Convention states “in which armed forces are engaged in conflicts,” but its preventive rationale applies equally to outside warfare [35]. Applying to this autonomous system, follows the implementation of fail-safe mechanisms, cybersecurity safeguards, and human-in-the-loop protocols to prevent algorithmic errors or malicious repurposing [37].

# Debris Avoidance in Low Earth Orbit

Jyoshika Barathimogan, Leow Eason, Helen Chen

While AI enhances real-time responsiveness and data interpretation, human operators retain ultimate responsibility for manoeuvre execution and mission-critical judgments. This approach addresses the “accountability gap” often associated with autonomous systems and strengthens compliance with established legal norms [36].

Furthermore, DAWN recognizes the dual-use nature of AI and satellite technologies, which may serve both civilian and military purposes. This duality necessitates clear regulatory definitions and operational boundaries to prevent misuse. The system therefore incorporates cybersecurity protocols and data transparency mechanisms that reduce the risk of interference or unlawful repurposing [37]. By aligning its design with the Geneva Conventions and the CCW’s guiding principles, DAWN ensures that its AI capabilities remain consistent with the broader objectives of peaceful and responsible space utilization.

DAWN’s ethical foundation are further reinforced by UNESCO’s Ethics of AI Recommendation (2021), which stresses that AI should support, not replace human judgment and NASA’s Framework for the Ethical Use of AI (2023), which emphasizes transparency, traceability, reliability, and governance oversight [36][38].

## Soft Law And Standardization in AI Governance

No binding treaties yet regulate AI use in space, but soft law frameworks and technical standards are closing that gap. These flexible, non-binding guidelines adapt quickly and often set the practical norms others follow. For DAWN, aligning with them builds credibility, trust, and international cooperation [39][40]. The ISO/IEC 42001:2023 standard defines how AI systems should be managed with transparency, fairness, and risk control. Likewise, the Consultative Committee for Space Data Systems (CCSDS) sets rules for communication and data exchange between satellites. By following these, DAWN ensures its AI systems are safe, traceable, and interoperable with other space missions [40].

Inspired by the Tallinn Manual, DAWN proactively embeds ethical and technical safeguards before binding regulations emerge. As Anne-Sophie Martin (2023) notes in “The Advent of AI in Space Activities: New Legal Challenges,” soft law offers a vital testing ground for responsible AI. It allows projects like DAWN to refine transparency and accountability before strict international laws exist [34].

## V. TRADE OFF ANALYSIS

Each design decision involves managing trade-offs between autonomy and oversight, efficiency and sustainability, and transparency and security. The following sections examine how DAWN navigates these competing priorities to achieve safe,

# Debris Avoidance in Low Earth Orbit

Jyoshika Barathimogan, Leow Eason, Helen Chen

sustainable, and trustworthy satellite operations.

## AI autonomy versus human control

DAWN faces a key trade-off between AI autonomy and human control. Greater autonomy enables faster responses, reduced reliance on ground stations, and quick action during collision risks. In Low Earth Orbit, even short communication delays can be critical. However, full autonomy brings risks. Without human oversight, AI may act unpredictably under data errors or sensor faults. The NASA Framework for the Ethical Use of AI (2023) warns of “automation complacency,” where humans place too much trust in machines.

To prevent this, DAWN follows a hybrid model grounded in MHC. Its AI, powered by Graph Neural Networks (GNNs) for debris prediction and Reinforcement Learning (RL) with Chance-Constrained Model Predictive Control (CC-MPC) for manoeuvre planning, generates recommendations but human operators approve final actions. This approach blends AI’s precision with human responsibility, ensuring DAWN’s missions remain transparent, safe, and aligned with OECD (2019) and UNESCO (2021) principles for ethical, human-centred AI.

## Efficiency versus Sustainability

A further trade-off emerges between the pursuit of immediate performance gains and DAWN’s long-term sustainability mission. High-performance manoeuvre algorithms may reduce short-term collision risk but can

accelerate fuel depletion, shortening a satellite’s operational lifespan. Likewise, overly frequent autonomous manoeuvres could introduce instability in orbital paths, complicating space traffic coordination.

DAWN resolves this through multi-objective optimization, integrating fuel efficiency, safety margins, and sustainability metrics into a single decision framework. The AI’s Reinforcement Learning component is explicitly trained to weigh these factors under uncertainty, prioritizing low-risk, fuel-efficient responses over aggressive manoeuvres. Furthermore, DAWN incorporates an end-of-life deorbit scheduler that identifies safe, low-congestion orbital windows for decommissioning, reducing long-term debris accumulation. It follows the ESA Zero Debris Charter (2023) and UNCOPUOS sustainability principles to ensure every move supports long-term safety in space.

## Transparency versus Security

DAWN’s ethical framework emphasises transparency in algorithmic decision-making. Explainable AI (XAI) enables operators to interpret and justify manoeuvre recommendations, reinforcing accountability and trust in autonomous operations. However, full transparency presents potential risks. Disclosing algorithmic logic or orbital data could expose the system to security threats or data misuse.

# Debris Avoidance in Low Earth Orbit

Jyoshika Barathimogan, Leow Eason, Helen Chen

To mitigate this, DAWN implements controlled transparency measures. Operational data are shared only within trusted networks compliant with ISO/IEC 27001 cybersecurity standards, while sensitive algorithmic information remains restricted to prevent exploitation. This measured approach ensures compliance with OECD (2019) and UNESCO (2021) principles, maintaining a balance between openness and security.

## VI. PRELIMINARY RESULT

### *Autonomous Debris Trajectory Prediction*

Initial simulations using Sentinel-1A orbital parameters demonstrate that the hybrid uncertainty-aware propagator substantially outperforms classical deterministic baselines. Across 100 Monte-Carlo trials under varying geomagnetic and solar flux conditions, the hybrid Graph-Bayesian model reduced the 24-hour position error by approximately 38% relative to SGP4 and 21% compared to the semi-analytic STELA propagator.

Performance gains were most pronounced during storm intervals ( $K_p \geq 5$ ), where learned drag correction layers maintained continuity in orbital state estimation. The integration of real-time space-weather indices further improved short-term forecast stability, yielding a mean RMSE below 1.2 km for low-Earth regimes below 800 km. These results validate the feasibility of on-board predictive adaptation under uncertain atmospheric regimes

### *Fuel-Optimal Manoeuvre Planning*

The reinforcement-learning-based manoeuvre planner achieved promising early performance in closed-loop simulation. Using a PPO-based policy network trained on perturbed encounter geometries, the agent consistently converged to near-optimal thrust sequences within the specified  $\Delta v$  budget. Compared with heuristic Lambert-targeting and convex-QP solvers, the RL agent achieved a **7–10% reduction in total fuel consumption** while maintaining comparable terminal miss distance (< 50 m) and compliance with collision probability thresholds ( $Pr(\text{collision}) \leq 10^{-4}$ ).

The trained policy exhibited strong generalisation to unseen debris conjunctions, adapting thrust duty cycles efficiently during eclipse transitions. The resulting trajectories remained dynamically feasible and respected on-board power and attitude constraints, confirming the planner's ability to negotiate both fuel efficiency and safety margins autonomously.

### *On-Board Object Classification*

Early flight-equivalent tests using synthetic and publicly available space-object imagery indicate robust classification accuracy under tight compute budgets. The multi-branch MobileViT-TCN architecture achieved a **macro-F1 of 0.91** across six operational object classes (payload, upper-stage, debris-fragment, tumbling debris, active satellite, unknown), outperforming single-branch CNN baselines by 8–12 points.

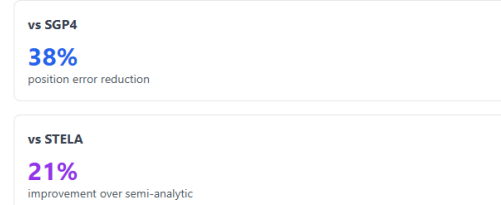
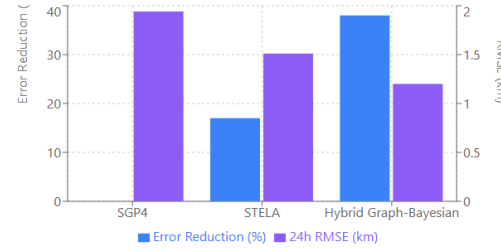
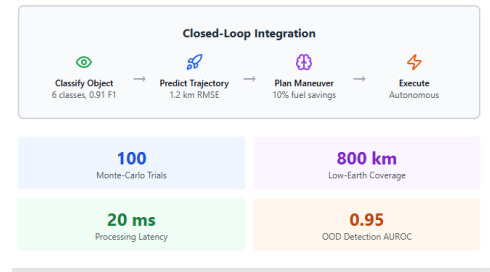
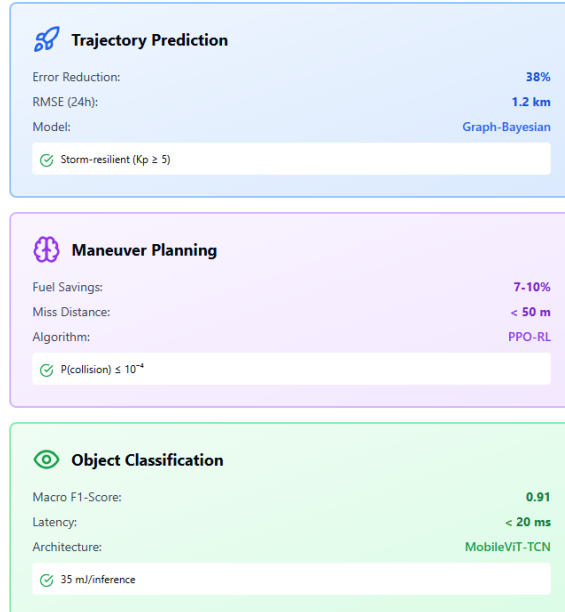
Latency remained below **20 ms per frame** on the emulated on-board processor (ARM-A76, 1 GHz) with energy

# Debris Avoidance in Low Earth Orbit

Jyoshika Barathimogan, Leow Eason, Helen Chen

consumption under **35 mJ/inference**, satisfying real-time constraints. The inclusion of photometric-curve and kinematic features improved discrimination between active and passive bodies, while the uncertainty head maintained reliable out-of-distribution rejection (AUROC > 0.95). These results confirm the classifier's viability for on-orbit inference within the autonomous control loop.

Collectively, the three subsystems show strong preliminary promise toward full closed-loop autonomy. The models achieve measurable improvements in accuracy, fuel efficiency, and computational viability without exceeding on-board resource budgets, establishing a credible technical foundation for integrated flight-test simulation.



# Debris Avoidance in Low Earth Orbit

Jyoshika Barathimogan, Leow Eason, Helen Chen

## On-Board Object Classification



### Macro F1-Score

**0.91**

8-12 pts vs CNN baseline

### Processing Latency

< 20 ms

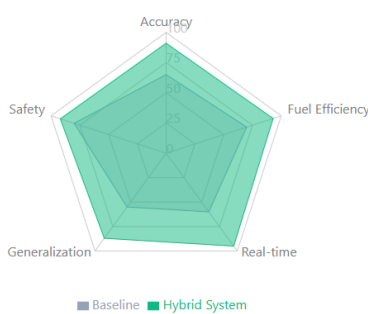
per frame on ARM-A76

### Energy Efficiency

< 35 mJ

per inference

## Integrated System Performance



### System-Level Achievements



#### Resource Efficiency

On-board compute, power, and fuel budgets satisfied



#### Safety Compliance

Collision probability and constraint adherence verified



#### Autonomy Ready

Three subsystems demonstrate closed-loop viability



#### Real-Time Capable

Latency and inference times within operational limits

## VII. PROJECT MANAGEMENT AND EXPECTED BUDGET

The project follows a modular development framework integrating three concurrent workstreams:

- (1) Trajectory Prediction,
- (2) Manoeuvre Planning, and
- (3) On-Board Classification.

Each sub-team operates under a unified Systems Integration Lead who oversees interface definition, data standardisation, and simulation consistency. Agile sprints are conducted bi-weekly, with milestones aligned to subsystem deliverables: algorithm design (Month 1), simulation validation (Month 2–3), and integrated end-to-end testing (Month 4). Continuous integration pipelines ensure reproducibility of on-board inference and control tests within the mission sandbox.

Risk management is handled through weekly technical reviews assessing computational constraints, sensor availability, and failure-mode simulations. Major decisions such as architecture changes, mission scenarios, or model retraining that follow a documented change-control process to maintain traceability and accountability.

## Resource Allocation and Responsibilities

### 5.2 Resource Allocation and Responsibilities

Workstream	Lead Responsibility	Core Deliverables
Debris Prediction	GNN/Graph-Bayes modelling, drag correction module	Hybrid uncertainty-aware orbit propagator
Fuel-Optimal Planning	Reinforcement-learning policy training, CC-MPC interface	PPO-based manoeuvre policy with constraint satisfaction
Object Classification	MobileViT-TCN pipeline, on-board feature fusion	Real-time classification engine with OOD detection
Systems & Integration	Firmware, telemetry bus, on-board scheduler	Closed-loop autonomy validation on Sentinel-1A simulator

# Debris Avoidance in Low Earth Orbit

Jyoshika Barathimogan, Leow Eason, Helen Chen

All workstreams report to the Mission AI Integration Team, ensuring coordination with the spacecraft's Guidance, Navigation, and Control (GNC) subsystem and communications interface.

## Expected Budget

The proposed budget covers development, simulation, hardware emulation, and validation over a four-month cycle. Cost estimates are derived from current ESA/NASA open-spec components and institutional computing resources.

Category	Description	Estimated Cost (SGD)
On-board Compute Prototype	NVIDIA Jetson Orin NX / equivalent flight-class SBC, radiation-tolerant enclosure	\$2,400
Sensor Emulation	Star-tracker, CMOS event-camera mockup, S-band RCS transceiver	\$1,800
Ground Simulation Hardware	GPU workstation (shared) for training & validation	\$1,500
Software & Licences	Orbital dynamics libraries, PyTorch/TensorRT optimisations, MATLAB test scripts	\$600
Testing & Integration	Power/thermal test bench, connector interfaces, cabling	\$900
Miscellaneous & Contingency (10%)	Logistics, replacements, consumables	\$900
Total Estimated Budget:		≈ \$8,100 SGD

Most computational resources (HPC nodes and storage) are institutionally provided, reducing total project expenditure. The estimated cost remains well within typical ISC mission research constraints.

## Timeline Overview

Month	Milestone	Key Output
Month 1	Architecture finalisation & dataset integration	Baseline models for all modules
Month 2	Mid-phase simulations	Preliminary metrics & cross-validation
Month 3	Hardware-in-loop testing	Real-time inference validation
Month 4	Integrated demonstration	End-to-end autonomous mission simulation

# Debris Avoidance in Low Earth Orbit

Jyoshika Barathimogan, Leow Eason, Helen Chen

## References

- [1] Nicholas, J. (2009b, October 16). *The collision of Iridium 33 and Cosmos 2251: the shape of things to come*. NASA Technical Reports Server (NTRS). <https://ntrs.nasa.gov/citations/20100002023>
- [2] David, L. (2021b, November 17). China's Anti-Satellite Test: Worrisome Debris Cloud Circles Earth. *Space*. <https://www.space.com/3415-china-anti-satellite-test-worrisome-debris-cloud-circles-earth.html>
- [3] The European Space Agency. (2016, August 31). *Copernicus Sentinel-1A satellite hit by Space Particle*. <https://www.esa.int>. Retrieved October 11, 2025, from [https://www.esa.int/Applications/Observing\\_the\\_Earth/Copernicus/Sentinel-1/Copernicus\\_Sentinel-1A\\_satellite\\_hit\\_by\\_space\\_particle](https://www.esa.int/Applications/Observing_the_Earth/Copernicus/Sentinel-1/Copernicus_Sentinel-1A_satellite_hit_by_space_particle)
- [4] Ecosystem, C. D. S. (2025c, August 25). Sentinel-1A data unavailability since 10 08 2025 (UPDATE). *Copernicus Data Space Ecosystem*. <https://dataspace.copernicus.eu/news/2025-8-11-sentinel-1a-data-unavailability-10-08-2025-update>
- [5] Ecosystem, C. D. S. (2025c, April 14). Copernicus Sentinel-1A Data unavailability on 1 April 2025. *Copernicus Data Space Ecosystem*. <https://dataspace.copernicus.eu/news/2025-4-2-copernicus-sentinel-1a-data-unavailability-1-april-2025>
- [6] *Sentinel Event Viewer | Copernicus Dashboard by ESA*. (n.d.). Copernicus Dashboard. <https://operations.dashboard.copernicus.eu/events.html>
- [7] Tulczyjew, L., Myller, M., Kawulok, M., Kostrzewska, D., & Nalepa, J. (2021). Predicting risk of satellite collisions using machine learning. *Journal of Space Safety Engineering*, 8(4), 339–344. <https://doi.org/10.1016/j.jssse.2021.09.001>
- [8] Massimi, F., Ferrara, P., & Benedetto, F. (2023). Deep Learning Methods for Space Situational Awareness in Mega-Constellations Satellite-Based Internet of Things Networks. *Sensors*, 23(1), 124. <https://doi.org/10.3390/s23010124>
- [9] Peter, H., Jäggi, A., Fernández, J., Escobar, D., Ayuga, F., Arnold, D., Wermuth, M., Hackel, S., Otten, M., Simons, W., Visser, P., Hugentobler, U., & Féménias, P. (2017). *Sentinel-1A – First precise orbit determination results*. *Advances in Space Research*, 60(5), 879–892. <https://doi.org/10.1016/j.asr.2017.05.034>
- [10],[11],[12],[13],[14],[15] *S1 Mission*. (n.d.). <https://sentiwiki.copernicus.eu/web/s1-mission>
- [16] [Geoinformatics, A. O. S. (2025, June 17). *Synthetic Aperture Radar*. GISRSStudy. <https://gisrsstudy.com/synthetic-aperture-radar/>
- [17],[18] *S1 Mission*. (n.d.). <https://sentiwiki.copernicus.eu/web/s1-mission>
- [19] *Two-line element set explained*. (n.d.). [https://everything.explained.today/Two-line\\_element\\_set/](https://everything.explained.today/Two-line_element_set/)
- [20] Ly, D., Lucken, R., Giolito, D., Share My Space, & Laboratoire de Physique des Plasmas (LPP), UMR CNRS 764, Ecole Polytechnique. (2019). Correcting TLES at EPoch: Application to the GPS constellation. In *First International International Orbital Debris Conference* [Conference-proceeding]. <https://www.hou.usra.edu/meetings/orbitaldebris2019/orbital2019paper/pdf/6132.pdf#:~:text=However%20TLES%20accuracy%20at%20epoch%20is%20typically%20large,rare%20too%20coarse%20to%20enable%20collision%20avoidance%20maneuvers>
- [21] *Detect space debris better with higher transmitting power*. (n.d.-b). Fraunhofer Institute for High Frequency Physics and Radar Techniques FHR. <https://www.fhr.fraunhofer.de/en/sections/Radar-for-Space-Situational-Awareness-RWL/Detect-space-debris-better-with-higher-transmitting-power-jb2021.html>
- [22] Limiting future collision risk to spacecraft. (2011c). In *National Academies Press eBooks*. <https://doi.org/10.17226/13244>
- [23] Szondy, D. (2020c, September 11). NASA straps a new space debris sensor onto the ISS. *New Atlas*. <https://newatlas.com/nasa-space-debris-sensor/52805/>
- [24] Anz-Meador, P., Ward, M., Manis, A., Nornoo, K., Dolan, B., Jacobs, HX5 – Jacobs JETS Contract, & GeoControl Systems – Jacobs JETS Contract. (2021d). The Space Debris Sensor Experiment. *The Space Debris Sensor Experiment*. <https://ntrs.nasa.gov/api/citations/20190033909/downloads/20190033909.pdf>
- [25] Guimarães, M., Soares, C., & Manfletti, C. (n.d.). *Predicting the properties of resident space objects in LEO using graph neural network*. <https://doi.org/10.17226/13244>
- [26] Ryu, K., Bouvier, J.-B., Lalani, S., Eggli, S., & Mehr, N. (2024, December 23). *Risk-sensitive orbital debris collision avoidance using distributionally robust chance constraints*. arXiv. <https://arxiv.org/pdf/2412.1735>

# Debris Avoidance in Low Earth Orbit

Jyoshika Barathimogan, Leow Eason, Helen Chen

- [27] Acciarini, G., Baydin, A. G., & Izzo, D. (2024). Closing the gap between SGP4 and high-precision propagation via differentiable programming. *Acta Astronautica*, 226, 694–701.  
<https://doi.org/10.1016/j.actaastro.2024.10.063>
- [28] Sanchez-Hurtado, S., Parker, W. E., Rodriguez-Fernandez, V., Linares, R., Universidad Polit cnica de Madrid, & Massachusetts Institute of Technology. (2025). FROM SPACE WEATHER TO ORBITS: AN UNCERTAINTY-AWARE FRAMEWORK FOR PREDICTING SATELLITE TRAJECTORIES. In *9th European Conference on Space Debris*. ESA Space Debris Office.  
<https://conference.sdo.esoc.esa.int/proceedings/sdc9/paper/377/SDC9-paper377.pdf>
- [29] Mueller, J., “Onboard Planning of Collision Avoidance Maneuvers Using Robust Optimization,” AIAA Infotech@Aerospace, Conference, American Institute of Aeronautics and Astronautics, Reston, Virginia, 2009.  
<https://doi.org/10.2514/6.2009-2051>
- [30] Solomon, A., & Paduraru, C. (2025). Collision avoidance and return manoeuvre optimisation for Low-Thrust satellites using reinforcement learning. *Proceedings of the 14th International Conference on Agents and Artificial Intelligence*, 1009–1016.  
<https://doi.org/10.5220/0013249000003890>
- [31] Anz-Medor, P., Ward, M., Manis, A., Nornoo, K., Dolan, B., Jacobs, HX5 – Jacobs JETS Contract, & GeoControl Systems – Jacobs JETS Contract. (2021b). The Space Debris Sensor Experiment. *The Space Debris Sensor Experiment*.  
<https://ntrs.nasa.gov/api/citations/20190033909/downloads/20190033909.pdf>
- [32] United Nations. (1967). *Treaty on principles governing the activities of states in the exploration and use of outer space, including the Moon and other celestial bodies (Outer Space Treaty)*. United Nations.
- [33] United Nations. (1972). *Convention on international liability for damage caused by space objects (Liability Convention)*. United Nations.
- [34] Martin, A.-S. (2023). *The advent of AI in space activities: New legal challenges*. *Journal of Space Law*, 49(2), 101–125.  
<https://www.semanticscholar.org/paper/The-Advent-of-Artificial-Intelligence-in-Space-New-Martin-Freeland/abe873ca25e22f65d943f37da324626cdd00bbd6>
- [35] United Nations. (1980). *Convention on certain conventional weapons (CCW)*. UN Treaty Series.
- [36] UNESCO. (2021). *Recommendation on the ethics of artificial intelligence*. Paris, France: United Nations Educational, Scientific and Cultural Organization.
- [37] International Organization for Standardization. (2022). *ISO/IEC 27001: Information security management systems – Requirements*. Geneva, Switzerland: Author.
- [38] National Aeronautics and Space Administration (NASA). (2023). *Framework for the ethical use of artificial intelligence*. Washington, DC: NASA Office of Technology, Policy and Strategy.
- [39] International Organization for Standardization. (2023). *ISO/IEC 42001: Artificial intelligence management systems – Requirements*. Geneva, Switzerland: Author.
- [40] Ryu, K., Bouvier, J.-B., Lalani, S., Eggli, S., & Mehr, N. (2024, December 23). *Risk-sensitive orbital debris collision avoidance using distributionally robust chance constraints*. arXiv. <https://arxiv.org/pdf/2412.17358>

## Image reference

European Space Agency. (n.d.). *Copernicus Sentinel-1A* [Image]. Credits: Thales Alenia Space – Italy (TAS-I). ESA. <https://www.esa.int/>

Kim, E., Han, S., & Al Sayegh, A. M. (2019). *Conceptual diagram to show the definition of the radial, in-track, cross-track (RIC) frame* [Image]. In *Sensitivity of the Gravity Model and Orbital Frame for On-board Real-Time Orbit Determination: Operational Results of GPS-12 GPS Receiver*. ResearchGate.  
[https://www.researchgate.net/figure/Conceptual-diagram-to-show-the-definition-of-the-radial-in-track-cross-track-RIC-fig1\\_334103287](https://www.researchgate.net/figure/Conceptual-diagram-to-show-the-definition-of-the-radial-in-track-cross-track-RIC-fig1_334103287)

Arzel, L. (2015, January 29). *Shining light on ATV* [Image]. ESA. <https://blogs.esa.int/orion/2015/01/29/shining-light-on-atv/>

RF Wireless World. (n.d.). *X Band frequency: Values, advantages, and applications* [Image].  
[https://www.rfwireless-world.com/terminology/x-band-frequency#google\\_vignette](https://www.rfwireless-world.com/terminology/x-band-frequency#google_vignette)

European Space Agency. (n.d.). *European Data Relay Satellite System (EDRS)* [Image].  
<https://www.eoportal.org/satellite-missions/edrs>

Sharp Energy Solutions Corporation. (n.d.). *Triple-junction (InGaP/GaAs/InGaAs) solar cell sheet (glass type)* [Image].  
<https://satsearch.co/products/sharp-energy-solutions-corporation-sesj-triple-junction-solar-cell-sheet-glass-type>

# Debris Avoidance in Low Earth Orbit

Jyoshika Barathimogan, Leow Eason, Helen Chen

European Space Agency. (n.d.). *Copernicus: Sentinel-1* [Image]. <https://www.eoportal.org/satellite-missions/copernicus-sentinel-1>

European Space Agency. (n.d.). *Satellite frequency band* [Image]. ESA. [https://www.esa.int/Applications/Connectivity\\_and\\_Secure\\_Communications/Satellite\\_frequency\\_bands](https://www.esa.int/Applications/Connectivity_and_Secure_Communications/Satellite_frequency_bands)

European Space Agency. (n.d.). *First image by Sentinel-1A C-SAR in SM dual polarization mode* [Image]. ESA. [https://www.esa.int/Applications/Observing\\_the\\_Earth/Copernicus/Sentinel-1/Highlights/Sentinel-1\\_first\\_images](https://www.esa.int/Applications/Observing_the_Earth/Copernicus/Sentinel-1/Highlights/Sentinel-1_first_images)

Copernicus: Sentinel-1 - eoPortal. (n.d.). *Sentinel-1A collision with space debris* [Image]. <https://www.eoportal.org/satellite-missions/copernicus-sentinel-1>

CelesTrak. (n.d.). *COSMOS 2251 debris* [TLE data]. <https://celesttrak.org/events/collision/>

National Research Council. (2011). *Orbital debris environment: Detection and monitoring*. In *Limiting future collision risk to spacecraft: An assessment of NASA's meteoroid and orbital debris programs* (pp. 17–22). The National Academies Press. <https://doi.org/10.17226/13244>

Gunter's Space Page. (n.d.). *SDS – Space Debris Sensor* [Image]. Retrieved October 12, 2025, from [https://space.skyrocket.de/doc\\_sdat/sds\\_iss.htm](https://space.skyrocket.de/doc_sdat/sds_iss.htm)

# **Debris Avoidance in Low Earth Orbit**

Jyoshika Barathimogan, Leow Eason, Helen Chen

This report has made use of Generative AI tools for selected sections as per ISC guidelines.

Tools used were chatgpt and claude to help assist in drafting and refining technical sections and formatting the report for clarity and conciseness. No non-critical or excessive reliance on Generative AI was employed; all technical content was reviewed, edited, and verified by the team.

## **Appendix B – Simulation Video**

<https://youtu.be/WCyEqc1U3gY>

## **Appendix C – Presentation Video**

[https://youtu.be/rmk\\_GgzPdd0](https://youtu.be/rmk_GgzPdd0)